

Review

Metabolic-based drug-drug interactions prediction, recent approaches for risk assessment along drug development

Xavier Boulenc¹ and Olivier Barberan^{2,*}

¹Drug Safety and Animal Research, Drug Disposition Domain, Sanofi Research and Development, Montpellier, France

²Product Development, Aureus Sciences, Paris, France

Abstract

Prediction of *in vivo* drug-drug interactions (DDIs) from *in vitro* and *in vivo* data, also named *in vitro in vivo* extrapolation (IVIVE), is of interest to scientists involved in the discovery and development of drugs. To avoid detrimental DDIs in humans, new drug candidates should be evaluated for their possible interaction with other drugs as soon as possible, not only as an inhibitor or inducer (perpetrator) but also as a substrate (victim). DDI risk assessment is addressed along the drug development program through an iterative process as the features of the new compound entity are revealed. Both *in vitro* and preclinical/clinical outcomes are taken into account to better understand the behavior of the developed compound and to refine DDI predictions. During the last decades, several equations have been proposed in the literature to predict DDIs, from a quantitative point of view, showing a substantial improvement in the ability to predict metabolism-based *in vivo* DDIs. Mechanistic and dynamic approaches have been proposed to predict the magnitude of metabolic-based DDIs. The purpose of this article is to provide an overview of the current equations and methods, the pros and cons of each method, the required input data for each of them, as well as the mechanisms (i.e., reversible inhibition, mechanism-based inhibition, induction) underlying metabolic-based DDIs. In particular, this review outlines how the methods (static and dynamic) can be used in a complementary manner during drug development. The discussion of the limitations and advantages associated with the various approaches, as well as regulatory requirements in that field, can give the reader a helpful overview of this growing area.

Keywords: CYP; drug-drug interactions; *in vitro in vivo* extrapolation.

Introduction

Over the last 15 years, drug-drug interactions (DDIs) have become one of the emerging topics in clinical drug development. Quantitative prediction of the *in vivo* DDIs caused by metabolic inhibition or induction, the most common DDI mechanisms in the clinic, has long been challenged. For drugs with narrow therapeutic indexes, the increase or decrease in plasma concentrations can, respectively lead to adverse effects or a loss of efficacy. The increase in exposure caused by DDIs can be substantial [e.g. the effect of ketoconazole on midazolam with an interaction ratio of 16-fold for the area under the plasma concentration-time curve (AUC) is a well-known example] in particular for substrates of CYP3A4 (Figure 1). Indeed, health authorities released dedicated guidelines in the late 1990s, recently updated (1, 2). In this context, simulations or predictions of DDIs bridging the gap between *in vitro* outcomes and clinical situations are challenging for the pharmaceutical industry, fueled by the recent growth of knowledge in molecular biology, computer-based simulation/predictions, and a better understanding of the inhibition and induction mechanisms. Quantitative prediction of DDIs is providing valuable information for increased efficiency in drug development and the avoidance of toxic interactions or loss of efficacy in clinical practice.

A drug can be considered as a “perpetrator” and/or a “victim.” A victim is a drug whose clearance is affected by a perpetrator. This last category refers to drugs (or other environmental factors) that inhibit or induce proteins (e.g., enzymes, transporters) responsible for clearing a victim drug. A pharmacokinetic drug interaction implies that a perpetrator causes a change in the clearance of the victim, in turn either decreasing or increasing concentrations of the victim drug in plasma and presumably at the site of action.

Most proteins (but certainly not all) to which drugs may bind are commercially available or readily produced in house; their role in pharmacokinetics can be isolated and assessed. Such tests include *in vitro* investigations to characterize a drug as a victim or a perpetrator toward drug-metabolizing enzymes, transporters, or plasma proteins. Quantitative metrics describing the interaction of the drug with the protein, such as binding constants, inhibition constants, and induction potential are part of this assessment and allow qualification of a drug as a potential victim and/or perpetrator toward a given enzyme/protein. It is generally accepted that all DDIs are graded depending on the concentrations of the interacting drugs (3). The magnitude of the interaction requires

*Corresponding author: Olivier Barberan, Product Development, Aureus Sciences, 174 Quai de Jemmapes, 75010 Paris, France
Phone: +33 1 40 18 57 53,
E-mail: olivier.barberan@aureus-sciences.com

Received September 20, 2011; accepted November 14, 2011

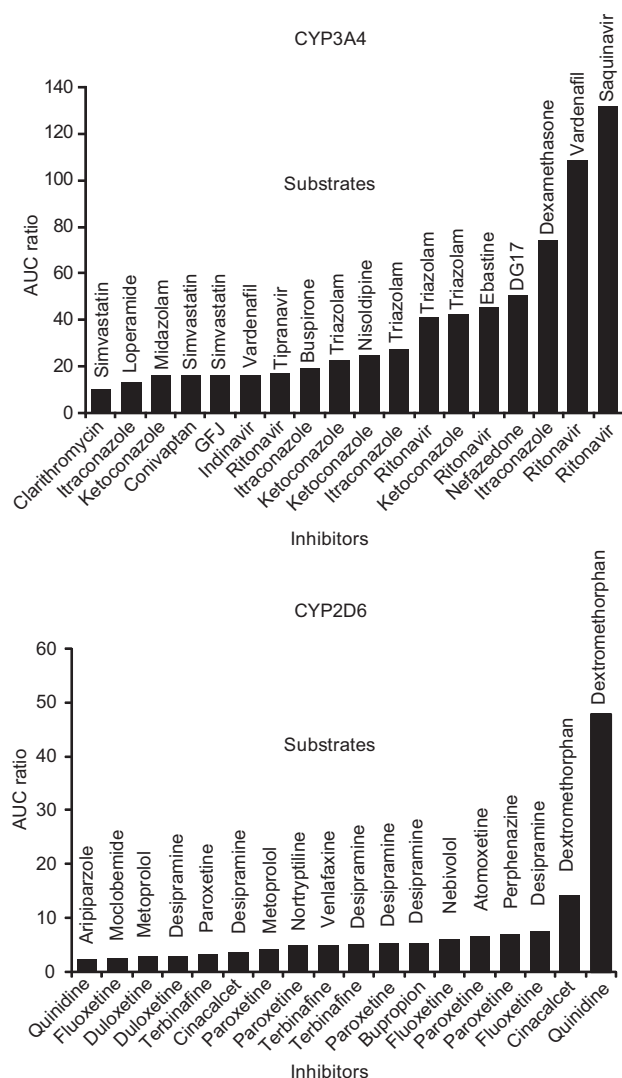


Figure 1 Highest interaction ratios for the two major CYP isoforms CYP3A4 and CYP2D6.

Source: AurSCOPE ADME/DDI database (June 2010 release).

mathematical models that have been proposed in the literature and that include several assumptions (4).

DDI prediction has been conceptualized to assist in drug development decisions. For that purpose, during the last 10 years major improvements for DDI prediction have been proposed, in particular for CYP450-based DDI, even though the former equations have never been considered as debatable (5). Thus, far, DDI predictions have been focused on metabolic drug interactions, but there are many pharmacokinetic DDIs other than those occurring at enzymatic sites, such as those involving transporters or altered physiological functions. As many drugs are highly bound to plasma and tissue proteins and with activity related to unbound drug, it is noteworthy that plasma protein-based DDIs, through displacement, were considered major concerns during the 1970s and 1980s. In practice, this concern is currently considered as unfounded in most cases (6).

During the last two decades, transporters have been identified as one of the major factors determining the pharmacokinetic properties of a drug; DDI predictions have been studied and are currently one of the expanding fields of investigations. This article mainly deals with metabolizing-enzyme drug-based DDI predictions, considering drugs as perpetrators (inhibitor and/or inducer) or victims (substrate of the inhibited or induced enzyme). Although not studied as extensively as the cytochrome P450 (CYP) enzymes, it is clear that other drug-metabolizing enzymes as well as transporters can play a major role in DDIs. In particular, even though transporters are out of the scope of this article, there is an increasing appreciation of the role that transporter proteins play in DDI.

In addition to the enzymes widely recognized as critical, CYP2C8 and CYP2B6 are also clinically relevant and should be included when assessing whether enzyme inhibition or induction has the potential to produce a drug interaction.

For the major CYPs involved in drug metabolism assessments of CYP metabolism, inhibition, and induction are generally determined as early as possible in the research and development stages. The mechanism of CYP inhibition [reversible or mechanism-based inhibition (MBI)] is a crucial factor to determine, and the result can potentially influence drug development strategies. This is why early prediction of the magnitude of clinical DDIs for compounds that have defined CYP inhibition and/or induction profiles is imperative to avoid potentially dangerous DDIs between compounds and putative comedication.

During the last decade or so, advances in our understanding of drug metabolism by CYP isoforms in particular and molecular mechanisms underlying DDIs have enabled guided risk assessments along drug development, improving the accuracy of the DDI forecast.

The purpose of this article is to provide an overview of the current equations and methods, the pros and cons of each method, the required input data for each of them as well as the mechanisms (i.e., reversible inhibition, MBI, induction) underlying metabolic-based DDIs. In particular, this review outlines how the methods [e.g., static, the concentration of the perpetrator is constant over time; dynamic, referring intrinsically to physiologically based pharmacokinetics (PBPK)] can be used in a complementary manner during drug development. The discussion of the limitations and advantages associated with the various approaches, as well as the regulatory requirements in that field, can give the reader a helpful overview of this growing area.

Simple static methods and authorities requirements

The first attempts to predict DDI considered simple equations separating the perpetrator and the victim.

The simplest approach applies to orally administered drugs undergoing linear “first pass” and “systemic” hepatic metabolism according to the “well-stirred” model. This model assumes that there is no transient plasma binding ($f_{u,b}$) displacement,

the fraction absorbed (F_a) and the hepatic blood flow (Q_H) are not modified by the presence of a perpetrator, and finally the concentration of the perpetrator does not change over time. Furthermore, the metabolism of the victim drug occurs only in the liver and metabolism is the only route of elimination.

Taking into account these considerations, the ratio of AUC with and without a perpetrator after oral administration of the victim drug at a dose (D) can be expressed as follows [Eq. 1]:

$$\frac{AUC_{po,i}}{AUC_{po}} = \frac{F_{a,i} \times F_{g,i} \times F_{H,i} \times \frac{D}{Cl_i}}{F_a \times F_g \times F_H \times \frac{D}{Cl}} = \frac{F_{H,i}}{F_H} \times \frac{Cl}{Cl_i} \quad [1]$$

where F_H and $F_{H,i}$ are the fractions of an oral dose escaping first-pass metabolism in the liver, and Cl and Cl_i are the total clearance in the absence and presence of an inhibitor, respectively. Because the well-stirred model apply, Eq. [1] could be expressed on the basis of hepatic blood flow (Q_H), unbound intrinsic clearance with ($Cl_{u,int,i}$) and without inhibitor ($Cl_{u,int}$), and unbound fraction in blood [Eq. 2]. Consequently, the AUC ratio after oral administration is directly proportional to the ratio of unbound intrinsic clearance with and without an inhibitor. Assuming that the victim is only metabolized by one enzyme, the inhibition of this pathway is competitive, and the concentration of the victim drug is lower than its Michaelis-Menten affinity constant ($[S] \ll K_m$), the change in AUC ratio is directly related to the well-known ratio $[I]/K_i$, where $[I]$ is the *in vivo* concentration of inhibitor and K_i is the inhibitory constant of the enzyme involved in metabolism of the victim drug [Eq. 3].

$$\frac{AUC_{po,i}}{AUC_{po}} = \frac{\frac{Q_H}{(Q_H + f_{u,b} \times Cl_{u,int,i})} \times \frac{Q_H \times f_{u,b} \times Cl_{u,int}}{(Q_H + f_{u,b} \times Cl_{u,int,i})}}{\frac{Q_H}{(Q_H + f_{u,b} \times Cl_{u,int})} \times \frac{Q_H \times f_{u,b} \times Cl_{u,int,i}}{(Q_H + f_{u,b} \times Cl_{u,int,i})}} = \frac{Cl_{u,int}}{Cl_{u,int,i}} \quad [2]$$

$$\frac{AUC_{po,i}}{AUC_{po}} = \frac{\frac{V_{max}}{K_m}}{\frac{V_{max}}{K_m \times \left(1 + \frac{[I]}{K_i}\right)}} = 1 + \frac{[I]}{K_i} \quad [3]$$

The same equation applies when the victim drug is a low clearance drug ($f_{u,b} \times Cl_{u,int} \ll Q_H$) administered intravenously (IV) (see mechanistic static model for general equation after IV route).

$$\frac{AUC_{iv,i}}{AUC_{iv}} = \frac{Cl_{u,int}}{Cl_{u,int,i}} = \frac{\frac{V_{max}}{K_m}}{\frac{V_{max}}{K_m \times \left(1 + \frac{[I]}{K_i}\right)}} = 1 + \frac{[I]}{K_i} \quad [4]$$

Some attempts have been made to predict clinical interactions with such simple equations (7, 8). Nevertheless, this

relationship cannot be considered for prediction as it relies on a major assumption that the victim drug is eliminated by a single metabolic pathway, which is not true in most cases (9). However, this approach is used for ranking inhibitors but cannot predict a specific DDI as most of the substrates are eliminated by multiple pathways and this is not taken into account. The pragmatic dimensionless ratio $[I]/K_i$ reflects the strength of inhibition of the compound for a given *in vivo* concentration. This is a useful predictive parameter, recommended by health authorities, for a given compound in order to qualify the inhibition risk toward CYP isoforms: the higher the ratio, the higher the risk. In other words, in the clinical setting, the inhibition of the isoform corresponding to the highest ratio allows to characterize the highest inhibition risk for a given clinical condition (dosage, administration route, dosing interval, etc.). Should no inhibition be observed (substrate probe AUC increase ≤ 2) with the highest potentially inhibited isoform, then no further clinical study will be warranted (Figure 2). If this first clinical study is positive, the next most potentially inhibited isoform must be investigated, and so on, until no interaction is observed. Conversely, assessing this simple ratio is also useful to rank compounds for a given isoform, in particular at the discovery level before entering development in order to select the compound reflecting the lowest inhibition risk.

In addition to this relative approach, this simple equation can be used for an absolute risk assessment. A value >0.1 is considered positive, reflecting a potential inhibition risk in the current Food and Drug Administration (FDA) guidance (1) as well as in the scientific community (10). A first absolute risk assessment can be performed with this ratio, considering the threshold value of 0.1 as recommended in the authorities guideline.

The FDA recommends considering total C_{max} as a conservative estimate of the *in vivo* concentration of the inhibitor ($[I]$) to avoid any false negatives. Using the same simple equation for reversible inhibition, the European Medicines Agency (EMA) authority considers the unbound maximal concentration (i.e., $C_{max,u}$) observed at the highest dose, with a threshold

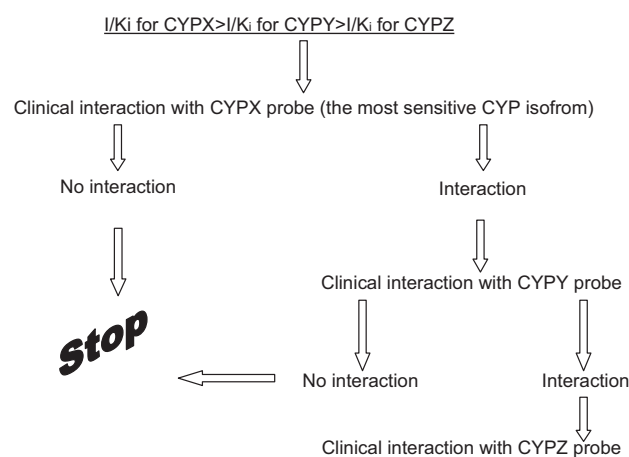


Figure 2 Rank order strategy for clinical studies to be conducted. The compound is tested as the perpetrator for three CYP isoforms with increasing risk of inhibition $X > Y > Z$.

value of 50; this threshold is 250 for highly bound drugs (i.e., >99%) to overcome any misleading value of calculated unbound C_{\max} (2) due to the variability linked with estimating the unbound drug fraction for such highly bound compounds. For interaction at the gut level, the intestinal concentration of the perpetrator is estimated assuming dose and an efficient volume of 250 mL, with a threshold value of 10.

Regarding mechanism based inhibitor (MBI) or time dependent inhibitor (TDI), a corresponding equation to Eq. [4] has been proposed [Eq. 5] (11). It assumed that the change in the steady-state concentration of the affected enzyme ($[E]_{ss}$) with and without a perpetrator is proportional to the change of intrinsic clearance. Consequently the following relationship applies:

$$\frac{AUC_{po,i}}{AUC_{po}} = \frac{Cl_{u,int}}{Cl_{u,int,i}} = \frac{[E]_{ss}}{[E]_{ss,i}} = \frac{\frac{R_{syn}}{k_{deg}}}{\frac{R_{syn}}{(k_{deg} + \lambda)}} = \frac{k_{deg} + \left(\frac{[I] \times k_{inact}}{[I] + K_i} \right)}{k_{deg}} \quad [5]$$

$$= 1 + \frac{k_{inact}}{k_{deg}} \times \frac{1}{1 + \left(\frac{[I]}{K_i} \right)}$$

where R_{syn} and k_{deg} are the synthesis rate and degradation rate constants of the affected enzyme, respectively; λ is the rate of enzyme inactivation due to the MBI described by equation $\lambda = [I] \times k_{inact} / ([I] + K_i)$; k_{inact} is the maximal rate of enzyme inactivation *in vitro*; and K_i is the concentration of the inactivator to reach half the maximal inactivation rate.

Nevertheless, this equation, with two dimensionless ratios ($[I]/K_i$ and k_{inact}/k_{deg}), is to be used with caution. This is because of the level of uncertainty linked to the natural enzyme turnover k_{deg} (see "Fold change in intrinsic clearance").

For CYP3A4, for which the highest number of MBIs has been described, this parameter is still debated in the literature (12). Nevertheless, once k_{deg} is selected, a risk assessment can be proposed positioning the inhibitor on an abacus, knowing k_{inact} and $[I]/K_i$ (Figure 3).

From a regulatory point of view, the FDA considers that a simple decision tree is to be developed, as is the case for reversible inhibition, and recommends conducting a clinical interaction study, in case an MBI is discovered, whereas the EMA advises conducting a clinical study until a 30% reduction in clearance is expected (2, 13).

Whatever the mechanism of inhibition, it is generally recommended to consider unbound *in vivo* inhibitor concentrations as well as unbound K_i and K_i for a reversible and a nonreversible inhibition, respectively. (This hypothesis will be explained in more detail in the next section, "Perpetrator concentration at the enzyme site.")

For a substrate compound, the interaction ratio can simply be estimated using the following equation:

$$\frac{AUC_{po,i}}{AUC_{po}} = \frac{Cl_{u,int}}{Cl_{u,int,i}} = \frac{1}{1 - f_m(E)} \quad [6]$$

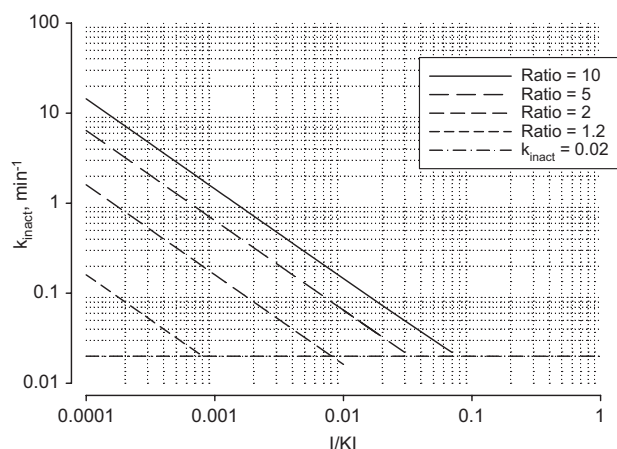


Figure 3 Abacus for MBI risk assessment, assuming $f_m(E)=1$ and $k_{deg}=0.00016 \text{ min}^{-1}$.

The ratio represents the AUC ratio with and without coadministration of inhibitor. The threshold $k_{inact}=0.02 \text{ min}^{-1}$ corresponds to the accepted lowest detectable limit using the classical current *in vitro* method.

where $f_m(E)$ is the relative contribution of a given CYP isoform to the overall clearance or to the metabolic clearance if the compound is eliminated only through metabolism.

This basic equation assumes that inhibition is total (very high $[I]/K_i$ for reversible inhibition) and does not take into account intestinal first pass that might be important for a CYP3A4 substrate. Authorities (1) recommend to investigate and identify enzymes involved in each metabolic pathway (CYP phenotyping) representing >25% of the overall clearance [$f_m(E)=0.25$]. This value is calculated by taking into account all other clearance mechanisms: renal, biliary, etc., in addition to the metabolic clearance. Therefore, it is necessary to have a complete picture of the elimination pathways of the investigational compound (14). Generally, data obtained after administration of a radiolabeled compound to humans provide the definitive pieces of information on the routes of drug clearance.

In addition to the enzymes widely recognized as critical (CYP1A2, CYP2C9, CYP2C19, CYP2D6, and CYP3A), CYP2C8 and CYP2B6 are clinically relevant and should be included when assessing whether enzyme inhibition or induction has the potential to produce a drug interaction.

Mechanistic static model method

The mechanistic static model (MSM) approach to predict CYP drug interactions of orally administered drugs was described for the first time by Rowland and Matin (5) and adapted by Ito et al. (3) and Obach et al. (15), like the $[I]/K_i$ approach, based on the "well-stirred liver" model, with similar assumptions; however, it takes into account clearance pathways other than the inhibited pathway in the prediction of AUC change. Therefore, it is assumed that the victim is only metabolized in the liver (and in the intestine for oral administration), and

also that the perpetrator and the victim were given at the same time. The static model is based on the use of a single *in vivo* constant concentration of the inhibitor. It ignores transient plasma binding displacement of the victim during the absorption phase and time variant perpetrator concentration leading to a different extent of inhibition of substrate metabolism during the “first” and subsequent passes through the liver.

This model also assumes that the fraction of the victim absorbed (F_a), the hepatic blood flow rate (Q_h), and the fraction of drug unbound in the blood ($f_{u,b}$) do not change in the presence of the perpetrator.

Taking into account these considerations, the ratio of AUC with and without a perpetrator after administration of the victim drug can be derived from Eq. [1] as follows [Eq. 7]:

$$\frac{AUC_{po,i}}{AUC_{po}} = \frac{1}{f_h \times \sum_{k=1}^n \frac{f_m(E_k)_h}{\text{Fold change } Cl_{u,int,k}} + 1 - f_h \times \sum_{k=1}^n f_m(E_k)_h} \quad [7]$$

where f_h is the fraction of hepatic clearance, $f_m(E_k)_h$ is the fraction of victim clearance mediated by the inhibited metabolic pathway “k,” and $Cl_{u,int,k}$ is the intrinsic metabolic clearance of substrate for the pathway “k” in the liver.

The ratio of AUC estimated by using the Rowland equation [Eq. 7] takes into account only metabolism in the liver.

However, many enzymes are expressed in the human small intestine; that is, not only CYP enzymes (CYP3A4, CYP3A5, CYP1A1, CYP2C9, CYP2C19, CYP2D6 and CYP2J2) but also transporters (P-glycoprotein, MRP1 and MRP2) (out of the scope of this review). CYP3A4 is the most highly expressed in the small intestine, accounting for 80% of total P450s, followed by CYP2C9 (14%), CYP2C19 (2%), and CYP2J2 (1.4%) (16, 17). The total amount of CYP3A expressed in the human small intestine (65.7–70.5 nmol) represents approximately 1% of the hepatic estimated CYP3A (18). Furthermore, the contribution of the intestine to the magnitude of DDIs may be significant, considering the high concentrations of inhibitors that are reached in the gut lumen during absorption.

Intestinal inhibition was incorporated in the DDI prediction model as the ratio of the intestinal wall availability, in the presence and absence of the inhibitor (F_{gi} and F_g , respectively) by Rostami-Hodjegan and Tucker (19) and also by Obach et al. (15) and Wang et al. (20) Eq. [8].

$$\frac{AUC_{po,i}}{AUC_{po}} = \frac{F_{gi}}{F_g} \times \frac{1}{f_h \times \sum_{k=1}^n \frac{f_m(E_k)_h}{\text{Fold change } Cl_{u,int,k}} + 1 - f_h \times \sum_{k=1}^n f_m(E_k)_h} \quad [8]$$

This approach is applicable to both reversible and irreversible inhibition interactions and also induction (increase of clearance is to be considered in this case). The concept of change in clearance can also be applied to the determination of the ratio of the intestinal wall availability in the presence and absence of a perpetrator [see Eq. 9].

$$\frac{F_{gi}}{F_g} = \frac{1}{F_g + (1 - F_g) \times \frac{Cl_{int,gi}}{Cl_{int,g}}} \quad [9]$$

The F_{gi}/F_g ratio can be estimated in three different ways (21, 22): *in vivo* determination, maximal F_{gi}/F_g , and model-predicted F_{gi}/F_g as outlined below. The F_g control values can be determined by *in vitro* methods, considering the intestinal metabolic Cl_{int} , permeability, and natural villous blood flow (23, 24), and also *in vivo* after oral and IV administrations of the compound (25). The details of these methods are beyond the scope of this article.

Briefly, *in vivo* determination involves both an IV and an oral administration of a victim drug in the presence of an inhibitor. This method is less interesting than the others because of the poor availability of data sets and the difficulty to obtain them.

A second *in vivo* method has been proposed using grapefruit juice. A single administration of grapefruit juice is able to selectively inhibit intestinal but not hepatic CYP3A4 through the fluranocoumarins that it contains, which cause inhibition of the enzyme. Hence, the F_g of a CYP3A4 substrate can be determined by comparing the AUC after oral administration with and without grapefruit juice (23, 24).

The “worst-case” scenario is used, that is, maximal inhibition of intestinal CYPs resulting in $F_{gi}=1$, and therefore in a maximal F_g ratio equal to $1/F_g$. Maximal inhibition can be used as a pragmatic estimation of the F_{gi}/F_g ratio (21) mostly when perpetrators are potent competitive inhibitors or inactivators.

A model-predicted F_g ratio is obtained from the decrease in the intestinal intrinsic clearance in the presence of an inhibitor using the *in vitro* obtained inhibitory constant (competitive or mechanism based) and the estimated inhibitor concentration in the intestinal wall during the absorption phase (15, 19).

Finally, considering oral administration, metabolism in the liver and also in the gut must be determined for assessing DDIs, and a combined model was proposed by Fahmi et al. (26, 27) where the fold change of intrinsic clearance with and without a perpetrator for enzyme “k” is defined according to the net effect of competitive inhibition, inactivation, and induction that occurs in the liver and in the gut [Eq. 10].

$$\frac{AUC_i}{AUC} = \frac{1}{F_g + (1 - F_g) \times \left(\sum_{k=1}^n \frac{f_m(E_k)_g}{C_{g,k} \times M_{g,k} \times T_{g,k}} + 1 - \sum_{k=1}^n f_m(E_k)_g \right)} \times \frac{1}{f_h \times \sum_{k=1}^n \frac{f_m(E_k)_h}{C_{h,k} \times M_{h,k} \times T_{h,k}} + 1 - f_h \times \sum_{k=1}^n f_m(E_k)_h} \quad [10]$$

where $C_{h,k}$ and $C_{g,k}$ are the terms for reversible inhibition in the liver and in the gut, respectively, associated to enzyme “k” and assuming inhibition by multiple perpetrators, and where $[I_u]_{h/g,j}$ is the unbound concentration of perpetrator “j” at the enzyme site (liver or gut) and $K_{i,j}$ the unbound inhibition constant for perpetrator “j” obtained from *in vitro* studies after accounting for nonspecific binding.

$$C_{h,k} = 1 + \sum_{j=1}^p \frac{[I_u]_{h,j}}{K_{i,j} + [I_u]_{h,j}} \quad [11]$$

$$C_{g,k} = 1 + \sum_{j=1}^p \frac{[I_u]_{g,j}}{K_{i,j} + [I_u]_{g,j}} \quad [12]$$

$M_{h,k}$ and $M_{g,k}$ are the terms for time-dependent inhibition in the liver and in the gut, respectively, associated to enzyme “k” and assuming inhibition by multiple perpetrators, and where $[I_u]_{h/g,j}$ is the unbound concentration of perpetrator “j” at the enzyme site (liver or gut), $K_{i,j}$ is the inhibitor concentration at which half maximal inactivation rate is achieved, k_{inact} is the true first-order inactivation rate constant, and $k_{deg,h/g}$ is the natural degradation rate constant for the enzyme in the liver or in the gut.

$$M_{h,k} = 1 + \sum_{j=1}^p \frac{k_{inact,j} \times [I_u]_{h,j}}{k_{deg,h,j} \times ([I_u]_{h,j} + K_{i,j} + u_{k,j})} \quad [13]$$

$$M_{g,k} = 1 + \sum_{j=1}^p \frac{k_{inact,j} \times [I_u]_{g,j}}{k_{deg,g,j} \times ([I_u]_{g,j} + K_{i,j} + u_{k,j})} \quad [14]$$

$T_{h,k}$ and $T_{g,k}$ are the terms for induction in the liver and in the gut, respectively, associated to enzyme “k” and assuming induction by multiple perpetrators where $[I_u]_{h/g,j}$ is the unbound concentration of perpetrator “j” at the enzyme site (liver or gut), E_{max} is the maximal induction effect, $EC_{50,u}$ is the unbound concentration (hepatocyte) of inducer associated with half-maximum induction, and n is the Hill coefficient.

$$T_{h,k} = \frac{1}{1 + \sum_{j=1}^p \frac{E_{max,k,j} \times [I_u]_{h,j}^n}{[I_u]_{h,j}^n \times EC_{50,u}^n}} \quad [15]$$

$$T_{g,k} = \frac{1}{1 + \sum_{j=1}^p \frac{E_{max,k,j} \times [I_u]_{g,j}^n}{[I_u]_{g,j}^n \times EC_{50,u}^n}} \quad [16]$$

MSM has been widely used for oral administration, basically because this route is the most common and the equation is simpler. Even so, MSM can also be used for IV dosing.

The change in AUC of the victim after IV bolus administration (AUC_{iv}) and during IV infusion (C_{ss}) can be expressed by the following equation, if the dose or infusion rate is constant (3)

$$\frac{AUC_{iv,i}}{AUC_{iv}} = \frac{C_{ss,i}}{C_{ss}} = \frac{1}{f_h \times \frac{Cl_{hi}}{Cl_h} + 1 - f_h} \quad [17]$$

where f_h represents the fraction of the hepatic clearance in the total clearance, and Cl_h and Cl_{hi} represent the hepatic clearance without and with a perpetrator, respectively.

Prediction of DDIs after IV administration of the victim can be described by Eq. [17], but it remains poorly reported

in the literature. Nevertheless, predictions involving high and low clearance drugs have been addressed by Ito et al. (3).

For high clearance drugs ($E_h=1$), Cl_h is rate limited by the hepatic blood flow rate and the hepatic clearance in presence of the perpetrator (Cl_{hi}) is still rate limited ($E_{hi}=1$) therefore AUC ratio is equal to unity indicating no change in AUC and consequently no DDI.

For low clearance drugs ($E_h<1$), Cl_h and Cl_{hi} are described by the unbound intrinsic clearance of the victim without and with the perpetrator. If protein binding is not affected by the perpetrator, the AUC ratio can be estimated by Eq. [7].

High clearance drugs ($E_h=1$), having Cl_h rate limited by hepatic blood flow for the victim drug alone but for which hepatic clearance is no longer rate limiting in the presence of the perpetrator, are not addressed by the equation of Ito et al. (3). This phenomenon occurs mostly when perpetrator inhibition is so strong that the clearance of the victim becomes so small that it becomes considerably less than the hepatic blood flow ($E_{hi}<<1$) and can lead to significant DDIs (AUC ratio >2). For example, administration of ketoconazole at 400 mg once a day or administration of an inactivator, such as erythromycin at 500 mg twice a day fits into this category.

As described above, administration of a victim drug by the IV route is paradoxically more complex as the basal clearance value (E_h without inhibitor) has to be taken into account for DDI prediction. Consequently, an MSM has been developed [Eq. 18] to predict the change in AUC after IV administration by different groups (25, 28) on the basis of the following parameters: the fraction of hepatic blood clearance to the total blood clearance of the victim drug (f_h); the fraction of affected drug cleared by each enzyme [$f_m(E_k)$]; the intrinsic clearance values for each enzyme affected or not affected by the perpetrator, respectively; and the hepatic extraction ratio of the victim drug (E_H).

$$\frac{AUC_{iv,i}}{AUC_{iv}} = \frac{1}{\frac{f_h}{1-E_H} + 1 - f_h + \sum_{k=1}^n \frac{f_m(E_k)_h}{C_{h,k} \times M_{h,k} \times T_{h,k}} + 1 - \sum_{k=1}^n f_m(E_k)_h + E_H} \quad [18]$$

where $C_{h,k}$, $M_{h,k}$ and $T_{h,k}$ are the terms for reversible inhibition, MBI, and induction respectively, associated to enzyme “k” and assuming involvement of multiple perpetrators. See Eqs. [11], [13], and [15].

A sensitivity/error analysis of the model was performed by Kirby and Unadkat (28) to determine the boundaries (degree of inhibition or induction) at which ignoring the E_H of commonly used victim drugs results in a $>30\%$ error in the predicted AUC ratio. These boundaries indicate that for most victim drugs, inhibition interactions with $[I]/K_i$ between 0.5 and 9 and induction interactions of <3 -fold will be susceptible to $>30\%$ error in the AUC ratio if the E_H of the victim drug is ignored. Consequently, to accurately predict the IV AUC ratio for all induction DDIs irrespective of E_H of the victim drug

and for modest to potent inhibition DDIs, even when the E_H is moderate (>0.3), the model described above should be used.

Eighteen *in vivo* clinical studies retrieved from publications were used by Lopez et al. (25) to compare actual and predicted DDIs with [Eq. 18] and without [Eq. 7] the basal clearance value of the victim drug (E_H ranging from 0.01 to 0.63). Predicted values derived from Eq. [18], without considering the E_H of the victim drug, tend to overpredict DDIs, whereas values predicted with E_H are more accurate (root mean square error of 0.51 with E_H vs. 0.93 without). Of course, the magnitude of predicted DDIs with this model [Eq. 18] is closely related to values of $f_m(E)$, E_H , and f_h for the victim drugs and potency of perpetrators (Figure 4). For example, a compound that is highly cleared by the liver ($f_h=90\%$) has a hepatic extraction ratio close to 1, and that metabolized quasi-exclusively by a single enzyme [$f_m(E) \sim 0.9$] could be involved in significant DDIs (AUC ratio >2) when perpetrators are potent ($[I]/K_i=10$) or very potent ($[I]/K_i=100$) (Figure 4).

Fold change in intrinsic clearance

In the presence of competitive inhibition, the fold reduction in intrinsic hepatic clearance through inhibition of enzyme “k” by a perpetrator can be applied to the liver or the gut and will be determined by the unbound concentration of perpetrator(s) (in the liver or in the gut) and its associated unbound equilibrium dissociation constant (K_{iu}) [Eqs. 11 and 12], assuming perpetrators are acting through the same mechanism of inhibition.

The relationship between $[I]/K_i$ and fold reduction clearance (or AUC ratios), for several f_m values of the substrate, is illustrated Figure 5. Whereas the determination of perpetrator concentration in the liver or in the gut will be detailed in a dedicated section (“Perpetrator concentration at the enzyme site”), the way of measuring and determining inhibitory parameters (K_i , IC_{50}) is discussed below.

The HLM assay is accepted as the “gold standard” for *in vitro* DDI assessment as it is felt to be closest to the native enzyme environment without the batch variability, potential transporter involvement, and cell penetration complications associated with human hepatocytes. The use of heterologous expression systems is not without complications either. The stoichiometry between NADPH CYP reductase, cytochrome b5, and individual CYP enzymes is sometimes different between heterologous expression systems and microsomes. The HLM assay has been used by many authors, but extensively by the group of Walsky, to assess *in vitro* DDI involving CYP2B6 and CYP2C8 (29–31).

A complete overview of these methods can be found in specialized reviews (32, 33) or in regulatory guidance (1).

The inactivation of CYPs by reactive products that form heme, protein adducts, or a metabolic inhibitory complex is referred to as mechanism-based inhibition (MBI). MBI is characterized as an irreversible or quasi-irreversible inactivation of CYP, requiring synthesis of a new enzyme for recovery of activity. Time-dependent inhibition is generally involved in more complex DDIs than reversible competitive inhibition, as it can result in a more profound and prolonged effect than the therapeutic dose or exposure might suggest.

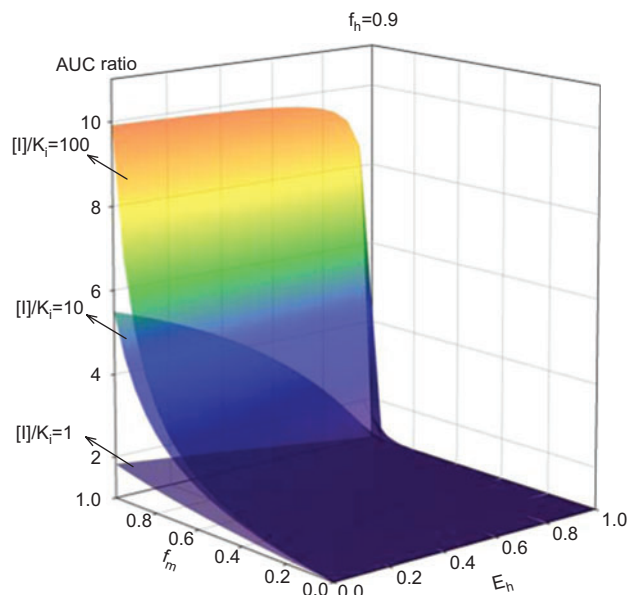


Figure 4 Three-dimensional surface plot for the relationship between the AUC ratio, E_H , and $f_m(E)$ based on Eq. [18] with three values of $[I]/K_i$ [low (1), medium (10), and high (100) competitive inhibitors] and $f_h=0.9$.

In the presence of inactivation, the fold reduction in intrinsic hepatic clearance will also be determined by the pseudo-first-order apparent inactivation rate (k_{obs}). This apparent inactivation rate is dependent on $[I]_{u,h/g}$ (unbound inhibitor concentration in the liver or the gut), K_{iu} (inhibitor concentration at which half maximal inactivation rate is achieved), and the true first-order inactivation rate constant (k_{inact}) [Eqs. 13 and 14].

Furthermore, the lack of information on *in vivo* turnover rates (k_{deg}) of several human CYP isoforms represents an important source of uncertainty in the *in vitro* *in vivo* extrapolation process. Determination of the rate constant of degradation in humans remains a challenge, even if determination in the liver has been completed for all the major CYP isoforms using the various techniques (32). Nevertheless, great variability

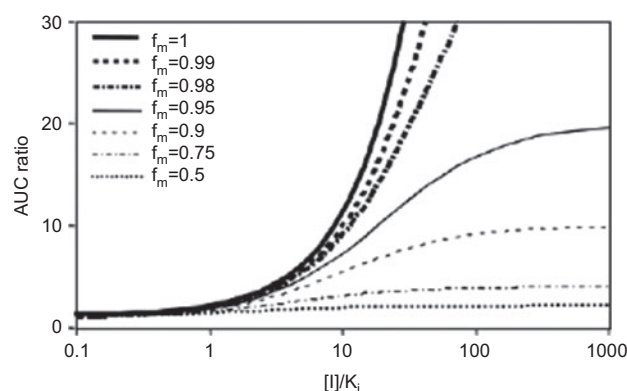


Figure 5 Effect of parallel pathways of drug elimination on predicted AUC ratio assuming a competitive inhibition.

has been observed that depends not only on the methods used but also on the sources of hepatocytes, for *in vitro* experiments and on patient populations for *in vivo* investigations. For example, the estimate of the average CYP3A4 half-life in the liver ranges from 26 to 140 h and was based on 13 determinations using *in vivo* and *in vitro* methods. Clearly, all *in vitro* methods will have some experimental deficiencies in reflecting the *in vivo* reality (12). Table 1 represents the common mean values of half-lives of degradation used for DDI prediction that have been obtained from literature analysis.

The common determination of MBI parameters (k_{inact} and K_I), also called conventional experimental protocol (CEP), was proposed by Silverman et al. (39) and involved two different experimental protocols with a common part that consists of preincubation of the enzyme and cofactors with different inhibitor concentrations for varying incubation times:

Followed by a dilution of the reaction mixture and further incubation of a probe substrate to assess the capability of the inactivator to block the active enzyme

Or without dilution but after a direct addition of a large amount of substrate probe to the preincubation mixture (40)

The calculation of k_{inact} and K_I uses the natural logarithm of the remaining enzyme activity plotted against the preincubation time according to Eq. [19]; the slopes of the initial log-linear phases represent the observed inactivation rate constants (k_{obs}).

$$k_{\text{obs}} = \frac{d[E]_t}{dt} / [E]_t = \frac{k_{\text{inact}} \times [I]}{K_I + [I]} \quad [19]$$

Two methods are generally used to obtain k_{inact} and K_I values; one is a linear method named after Kitz and Wilson (41) and the other is a non-linear regression method.

A modification of the CEP was proposed recently by Yang et al. (23, 24), named the mechanistically based experimental protocol. Since it uses CEP for characterizing MBI, it may introduce a substantial bias in estimating parameter values (42).

Table 1 Common mean hepatic values of half-lives of degradation used for DDI prediction, from literature analysis.

| Enzymes | $k_{\text{deg h}^{-1}}$ | References |
|---------|-------------------------|------------------------|
| CYP1A2 | 0.000296 | (11), (34) |
| CYP2B6 | 0.000361 | (11) |
| | 0.00026 | (34) |
| CYP2C19 | 0.000444 | (11) |
| | 0.00026 | (34) |
| CYP2D6 | 0.000226 | (11), (34), (35) |
| | 0.00024 | (36) |
| CYP3A4 | 0.000321 | (11), (26), (27), (34) |
| | 0.00016 | (32), (37) |
| | 0.00016–0.00050 | (36) |
| | 0.000769–0.00128 | (20) |
| | 0.0005 | (38) |
| CYP2C9 | 0.00026 | (34) |

Two other methods, generating IC_{50} values rather than k_{inact} , were used for identifying inactivators. These methods measure the decrease in IC_{50} values occurring through preincubation of the inhibitor with liver microsomes and NADPH (34, 43). The IC_{50} measured after such a preincubation was highly correlated with the k_{inact}/K_I ratio measured after a full characterization of inactivation. These methods were analyzed and compared (36) to establish potential usage in terms of *in vitro-in vivo* extrapolation.

In the presence of induction, the fold change in intrinsic clearance will also be determined by inducer concentrations at the enzyme site $[I_u]_{h,g}$ (in the liver or in the gut), the maximum fold induction (E_{max}), and the concentration of inducer associated with half-maximum induction (EC_{50}); however, how these three elements are combined can vary. To date, two predictive models exist for calculating fold reduction in intrinsic clearance based on an empirical calibration factor “d” [Eq. 20] (26, 44) or on a Hill equation (45) [Eqs. 15 and 16].

$$\text{Fold change Clint, } u_{h/g,k} = \frac{1}{1 + \sum_{j=1}^p \left(\frac{d \times E_{\text{max}} \times [I_u]_{h/g,j}}{[I_u]_{h/g,j} + EC_{50,j}} \right)} \quad [20]$$

The “d” parameter in Eq. [20] represents an empirical calibration factor for the purposes of *in vitro* to *in vivo* induction scaling. As such, its value is estimated through correlation of predicted and observed AUC ratios.

In many cases, E_{max} and EC_{50} are not readily obtained from concentration-response curves measured in *in vitro* induction assays because of limitations imposed by drug solubility, cell permeability, or toxicity. In these cases, the slope of the induction response curve (equivalent to E_{max}/EC_{50}) at a more experimentally feasible low concentration range of the inducer can be used for the prediction. This method [Eq. 21] is, however, only applicable if *in vivo* concentrations of an inducer are low ($[I]_{h,j} \ll EC_{50,j}$).

$$\text{Fold change Clu}_{\text{intk}} = \frac{1}{1 + \sum_{j=1}^p (\text{slope}_j \times [I_u]_{h,j}^n)} \quad [21]$$

An alternative approach was investigated by Ohno et al. (45). This method was developed using the principle that the extent of alterations in the AUC is predicted from *in vivo* information obtained from minimal clinical studies without using *in vitro* data. These authors determined the apparent CYP3A4 contribution to total oral clearance of the substrates from inhibitory DDI studies using a potent CYP3A4 inhibitor, such as itraconazole or ketoconazole. For drugs that are inducers, at a given dose and treatment duration, the apparent increase in clearance was calculated on the basis of the reduction of the AUC for standard CYP3A4 substrates, such as midazolam or simvastatin. For drug candidates, CYP3A4 involvement in the clearance can be determined from clinical studies with inhibitors or from *in vitro* investigations to predict the quantitative decrease in AUC after coadministration with a given inducer.

Parameters for victim drug-parallel pathway: fraction metabolized [$f_m(E)$]

Consideration of the fraction of total clearance of victim drug, mediated through the enzyme being inactivated [$f_m(E)$], is crucial when a risk assessment for interaction between a specific victim and perpetrator drug pair is evaluated. Determination of the f_m values is first determined *in vitro* reaction phenotyping (also known as enzyme mapping), although these values can be refined through consideration of clinical outcomes (see below).

The relationship between fold increase in AUC and the $f_m(E)$ of the victim drug is illustrated in Figure 5 for various values of the $[I]/K_i$ ratio. Obtaining initial estimates of $f_m(E)$ of the victim drug is not always straightforward. Fractions metabolized of the victim drugs are estimated by using *in vitro* or *in vivo* approaches.

In vitro approaches mainly involve reaction phenotyping of major metabolic pathways by using factors to scale to *in vivo* metabolic clearance from recombinant CYP experiments. The fraction metabolized for an enzyme [$f_m(E)_{\text{vitro}}$] is estimated by dividing the estimated clearance for this enzyme (different pathways) by the total *in vitro* clearance [Eq. 22]

$$f_m(E_i)_{\text{vitro}} = \frac{\sum_{k=1}^p Cl_{u,\text{int},k} (rE_i) \times SF_i}{\sum_{j=1}^n \left(\sum_{k=1}^p Cl_{u,\text{int},k} (rE_j) \times SF_j \right)} \quad [22]$$

where there are “j” enzymes with corresponding $Cl_{u,\text{int},k} (rE_i)$ values calculated from enzyme kinetic parameters for different pathways “k” in each recombinant system and where SF_j is a scaling factor corresponding to enzyme “j.”

When recombinant systems are used, an RAF is proposed as the scaling factor to allow for differences in enzyme activities per unit of microsomal protein, compared with that in HLMs (46).

Alternatively, enzyme abundance can be used as a scaling factor to estimate fraction metabolized *in vitro*, by the extrapolation of recombinant clearances to HLM clearances (47).

However, using enzyme abundance as a scaling factor does not allow for any difference in the variability of activity per unit amount of CYP between the expression system and the liver. Thus, Proctor et al. (48) proposed incorporating a scaling factor [intersystem extrapolation factor (ISEF)] in the abundance method to take into account different intrinsic activities in recombinant enzyme systems. ISEF is a dimensionless number used as a direct scaler to convert data obtained with a recombinant enzyme system into that of an HLM. As with RAF, the ISEF may be defined not only with respect to V_{max} but also to intrinsic clearance.

The second *in vitro* CYP reaction phenotyping method consists of using HLMs incubated with or without chemical inhibitors or inhibitory antibodies. In the case where a compound is metabolized by multiple CYP isoforms, a combinatorial approach with two or more inhibitors (or antibodies) may be considered (14).

For a polymorphic CYP isoform, genotyped/phenotyped HLM can be used. Clearance comparison between poor and extensive HLM metabolizers enables $f_m(E)$ determination as done *in vivo* [Eq. 23]. Instead of HLM, another more physiological *in vitro* material can be considered: human hepatocytes. The advantage of this last method over the others is the lack of necessity for scaling factors and the “more physiological” feature of the latter. Other tissue-based systems are sometimes used (e.g., liver tissue slice) with similar methods. Nevertheless, the lack of specificity of the inhibitors/antibodies is a concern, and complications may arise owing to differing effects on enzyme kinetics of various substrates and inhibitor concentrations. It is also worth noting that low-turnover compounds (low Cl_{int}), metabolized by more than two CYPs, are difficult to phenotype. It is particularly true with the HLM and hepatocyte methods, as in this case clearance differences with or without an inhibitor are difficult to assess.

A variety of *in vitro* systems can be used to evaluate the roles of different CYPs in the metabolic clearance of a victim, and each system has its own advantages and disadvantages. Therefore, it is often recommended to use more than one system and to integrate all of them to consider various aspects of the experimental design and the entire *in vitro* data set to make an assessment of the CYP reaction phenotype.

Instead of using *in vitro* experiments, *in vivo* approaches were applied to determine $f_m(E)$ -like phenotyping, chemical *in vivo* inhibition, non-linear regression, or renal excretion.

The simplest case is that of the polymorphic expression of the enzyme being inhibited with the existence of clearly definable extensive metabolizer (EM) and poor metabolizer (PM) populations, for example, CYP2D6, CYP2C9, or CYP2C19. The fraction metabolized by the polymorphic enzyme can be expressed by the following relationship [Eq. 23] involving EM and PM clearance or AUC (49)

$$f_m(E) = \left(1 - \frac{Cl_{\text{(PM)}}}{Cl_{\text{(EM)}}} \right) \times \frac{1}{1 - EF} = \left(1 - \frac{AUC_{\text{(EM)}}}{AUC_{\text{(PM)}}} \right) \times \frac{1}{1 - EF} \quad [23]$$

where the enzyme function (EF) is the ratio of polymorphic enzyme function in a PM relative to an EM subject. As described above, EF values >0 and <1 represent the degree of impairment in enzyme function resulting from the polymorphism.

In such cases, knowledge of the pharmacokinetics in EM vs. PM subjects will help define $f_m(E)$. For example, this approach was extensively and successfully used to estimate f_m (CYP2D6) (9) for a set of nine CYP2D6 victims (50) (EF=0).

Alternatively, initial estimates of $f_m(E)$ can be obtained from the results of clinical DDI studies with selective potent inhibitors of enzymes that essentially produce a complete inhibition of the enzyme of interest (*in vivo* chemical inhibition method). A total inhibition [$[I]/K_i \gg 1$ for competitive inhibition or $\frac{k_{\text{inact}} \times [I_u]_{h,j}}{k_{\text{deg,h}} \times ([I_u]_{h,j} + K_{Iu,j})} \gg 1$ for MBI] produces

a maximum possible AUC ratio that is solely dependent on $f_m(E)$ [Eq. 24]

$$f_m(E) = 1 - \frac{1}{AUC_{ratio}} = 1 - CI_{ratio} \quad [24]$$

A total inhibition is assumed when, for example, ketoconazole is administered at 400 mg/day for CYP3A4 or when paroxetine is administered at 30 mg/day for CYP2D6. This method was used by Ohno et al. (45, 51) to estimate the fraction metabolized of CYP3A4 victims by using ketoconazole or itraconazole as selective competitive inhibitors and diltiazem as the mechanism-based inactivator. A similar study on CYP3A4 was published by Shou et al. (52), including an extended list of inhibitors (troleandomycin, ritonavir, mibefradil, fluconazole, itraconazole, clarithromycin, saquinavir, erythromycin, and grapefruit juice). An estimate of 0.93 for contribution of CYP3A to the overall clearance of midazolam has been derived on the basis of an observed mean 16-fold increase in total exposure following administration of 400 mg/day ketoconazole (15).

A number of approaches exist for obtaining $f_m(E)$ values and are described above. The importance of considering $f_m(E)$ to predict accurate DDIs was emphasized by many authors not only for mechanism-based or competitive inhibition (9, 45, 53, 54) but also for induction (45). For example, when assuming competitive inhibition and only one inhibited pathway, determination of the absolute value of $f_m(E)$ is of great importance whether the particular enzyme under examination contributes to >50% of the total clearance. Despite the potency ($[I]/K_i$) of the inhibitor, a maximal AUC ratio of 2 is obtained when $f_m(E)$ is equal to 0.5. With a value of $[I]/K_i > 10$, a small increase in $f_m(E)$ will dramatically affect the AUC ratio. This phenomenon grows exponentially in conjunction with the increase of $f_m(E)$ (Figure 5). Consequently, accurate determination of $f_m(E)$ will be mandatory for an exact prediction of DDI.

If the use of $f_m(E)$ is not debatable, this is not the case for methods employed to determine values for a particular substrate. The general tendency when Figures 6 and 7 are observed is a significant variability of $f_m(E)$ values not only for CYP2D6 but also for CYP3A. For example, felodipine, a substrate of CYP3A4, has a maximum and minimum value of 0.99 and 0.81, leading to a maximum (assuming a total competitive inhibition $[I]/K_i \gg 1$) and a minimum AUC ratio of 100 and 5.26, respectively.

The *in vivo* situation is sometimes more difficult as total clearance and $f_m(E)$ values can vary, reflected by non-linear pharmacokinetics. Below are the three major clinical situations for which $f_m(E)$ values of the enzymes involved in a given compound can vary:

1. Saturation of one metabolic pathway: A single metabolic pathway can be saturated when increasing the dose whereby the overall clearance is decreased and all the $f_m(E)$ values are rearranged with $[f_m(E)$ values of the unsaturated pathways increased] (Figure 8).

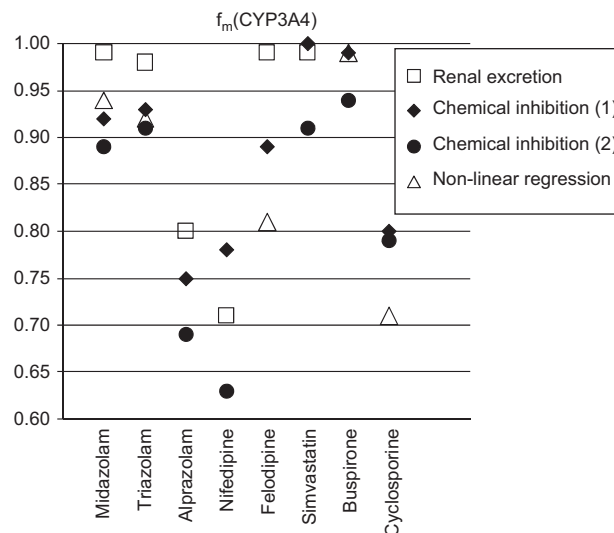


Figure 6 $f_m(CYP3A)$ values were collected from literature analysis using the AurSCOPE ADME/DDI database (December 2010 release) based on renal excretion, chemical inhibition, and non-linear regression.

2. Induction of one metabolic pathway: Conversely, the relative involvement of a given isoform can increase in case of induction; in this case, the overall clearance is increased and all other $f_m(E)$ values are also rearranged (decrease).
3. Genotyping: It is also worth noting that genetic polymorphism involving CYP genes has, of course, a tremendous impact not only on the $f_m(E)$ of polymorphic enzymes but also on the nonpolymorphic ones. In subjects who lack the major metabolic clearance pathway (PMs), the remaining pathway(s) become more important (Figure 9). Authorities

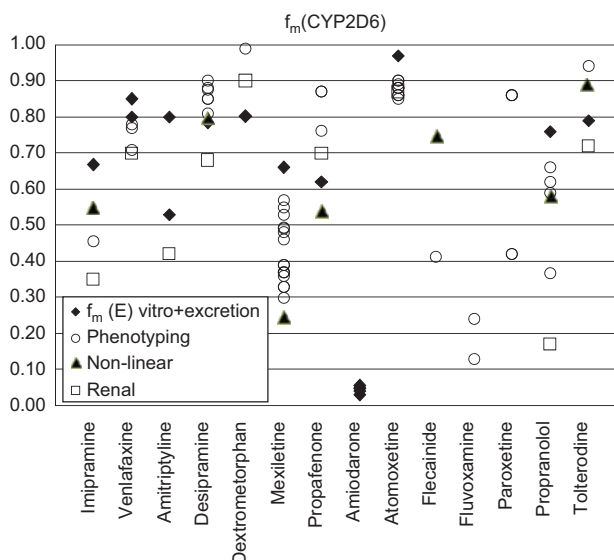


Figure 7 $f_m(CYP2D6)$ values were collected from literature analysis using the AurSCOPE ADME/DDI database (December 2010 release) based on renal excretion, non-linear regression, phenotyping, and *in vitro* determination methods.

recommend addressing these pathway(s) in these specific populations (1).

Perpetrator concentration at the enzyme site

[I] has been defined as the concentration of inhibitor at the enzyme site, which in practice is unmeasurable. One of the key challenges, however, is the estimation of the most appropriate value of [I]. Estimation of [I] is based on *in vivo* concentrations of a given perpetrator that change over time, raising the question of whether the systemic plasma concentration or the

hepatic inlet concentration is the most relevant concentration (Table 2).

In addition, the impact of plasma-protein binding remains controversial even though the use of total plasma systemic concentration has been advocated in the past as a means of predicting reversible-inhibition DDIs; however, this is contrary to the well-established “free-drug hypothesis” of drug action in DDI predictions. Do we take into account for the estimation of [I] the total plasma concentration or the unbound plasma concentration?

In most of the publications dealing with the impact of inhibitor concentration on the accuracy of DDI prediction (Table 3), correction taking into account the free drug fraction was shown to lead to the most accurate predictions, not only for MBIs but also for reversible inhibitor mechanisms. Nevertheless, it is essential to note that the total concentration was also determined by other authors (53, 57) as the best concentration leading to the more accurate DDI predictions.

Consideration of the systemic plasma concentration as opposed to the hepatic inlet concentration is also crucial. Most of the publications predicting DDIs involving reversible competitive inhibitors have determined that the hepatic inlet concentration ($[I]_{u, \text{in, avg}}$ or $[I]_{u, \text{in, max}}$) (Table 3) provided the most accurate DDI predictions, whereas prediction of DDIs involving MBI or induction mechanisms are more accurate when systemic unbound plasma concentration ($C_{\text{max, u}}$) is introduced in the calculations. This previous result was also supported by our unpublished results where it was found that using unbound systemic plasma concentrations ($C_{\text{max, u}}$ or $C_{\text{avg, u}}$) for the prediction of DDIs between the midazolam victim and eight inactivators of CYP3A4 increased the accuracy and significantly reduced the overprediction observed when the hepatic inlet concentrations were used ($[I]_{u, \text{in, avg}}$ or $[I]_{u, \text{in, max}}$) (Figure 10).

It was found that the reversible inhibition performed best when the unbound portal vein concentration was used for the concentration in the liver, whereas for irreversible inactivation and induction, the unbound systemic concentration was best. Even though these results appear inconsistent from a physiological point of view, they can be rationalized. For reversible inhibition, much of the interaction occurs during absorption and the hepatic first pass, after which perpetrator concentrations decrease below values required to exhibit reversible interaction. Consequently, the use of the hepatic inlet concentration for predicting DDIs makes sense when reversible inhibitors are involved.

Conversely for inactivation and induction, the use of systemic concentrations makes sense in that the DDIs caused by inactivators and inducers continue to occur after first-pass exposure of the intestine and liver is over.

Even though most of the predictive results can be rationalized, some are contradictory. For example, the total systemic plasma concentration (C_{avg}) was determined to be the concentration leading to the most accurate prediction for reversible competitive inhibitors (53, 57). These considerations may underline some limitations of the mathematical model.

Systemic or hepatic inlet concentrations can be entered into the mathematical model as total or unbound exposure.

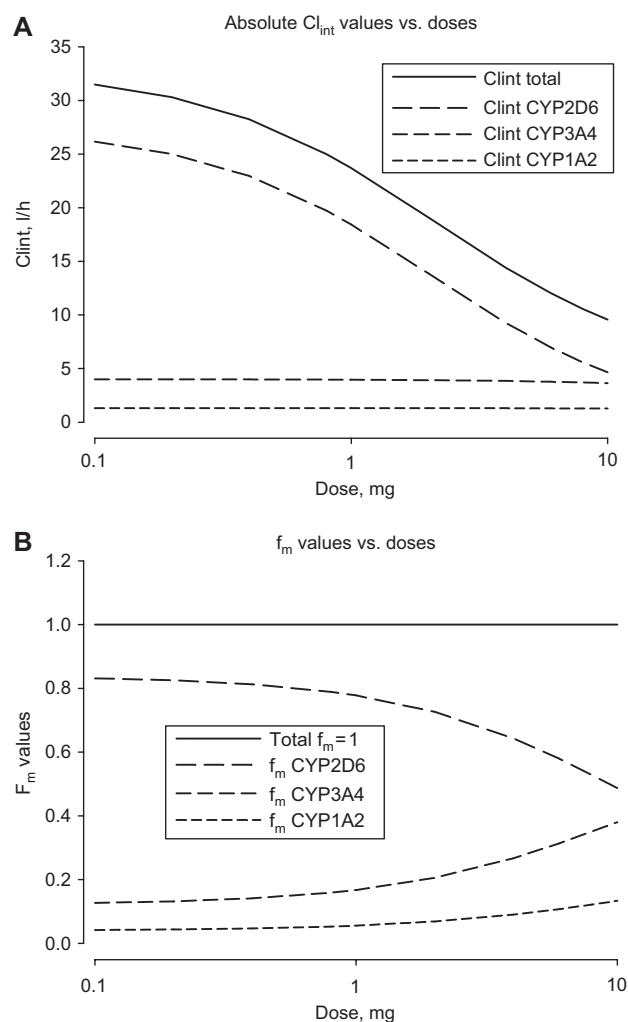


Figure 8 Absolute Cl_{int} (A) and corresponding f_m (E) values (B) for a compound metabolized by CYP1A2, CYP2D6, and CYP3A4 with a saturation of CYP2D6.

Data were simulated with the following V_{max} (pmol/min/pmol of CYP) and K_m (μM) parameter values: CYP2D6 ($K_m=0.2$; $V_{\text{max}}=5.6$), CYP1A2 ($K_m=32$; $V_{\text{max}}=43$), CYP3A4 ($K_m=10$; $V_{\text{max}}=40$). f_m (E) is calculated with Eq. [22]; each Cl_{int} value is calculated for each substrate concentration with $Cl_{\text{int}} = V_{\text{max}} / (K_m + [S])$ [see parallel pathway, f_m (E) calculation in this section]. For clearance calculation, concentration was assumed to be equal to the portal concentration with a fraction absorbed $F_{\text{abs}}=1$ and gut bioavailability $F_g=1$.

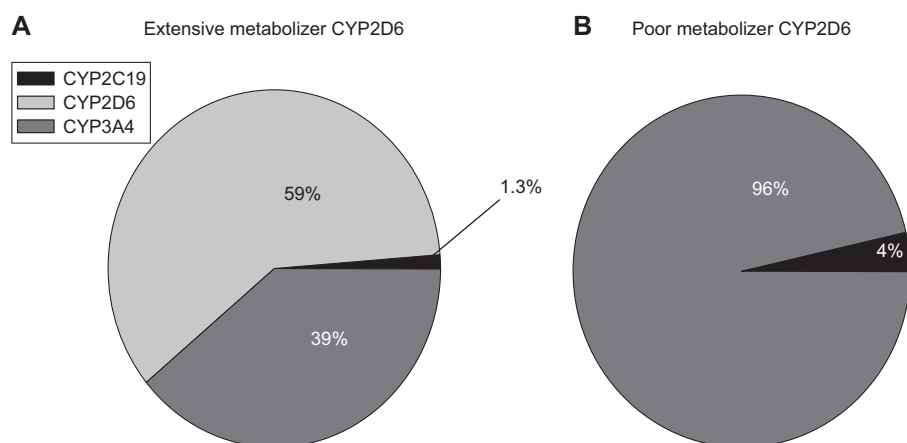


Figure 9 CYP3A4, CYP2D6, and CYP2C19 isoform relative contributions in intrinsic clearance of CYP2D6 EM (A) and PM (B) subjects for a substrate metabolized by these three enzymes.

Table 2 Consolidation of some methods for computing (and selecting) values for $[I]$ found in the literature for DDI prediction.

| Choice of $[I]$ | Estimation of $[I]$ |
|--|--|
| Maximum steady-state plasma concentration | $[I]_{\max} = C_{\max}$ |
| Unbound concentration | $[I]_{\max,u} = f_{u,b} \times C_{\max}$ |
| Average steady-state plasma concentration | $[I]_{\text{avg}} = C_{\text{avg}}$ |
| Unbound concentration | $[I]_{\text{avg},u} = f_{u,b} \times C_{\text{avg}}$ |
| Maximum hepatic inlet plasma concentration | $[I]_{\text{in,max}} = C_{\max} + \frac{F_{\text{abs}} \times k_{\text{abs}} \times D}{Q_h}$ |
| Unbound concentration | $[I]_{\text{in,max},u} = f_{u,b} \times [I]_{\text{in,max}}$ |
| Average hepatic inlet plasma concentration | $[I]_{\text{in,avg}} = C_{\text{avg}} + \frac{F_{\text{abs}} \times k_{\text{abs}} \times D}{Q_h}$ |
| Unbound concentration | $[I]_{\text{in,avg},u} = f_{u,b} \times [I]_{\text{in,avg}}$ |

It is common practice with such approaches to empirically select surrogate measures of exposure in the liver and intestine that provide the best correlation of predicted and observed DDIs reported in the literature.

Although practically useful, such empirical oversimplifications surely limit predictive accuracy within victims and perpetrators involved in the predictions, and it would be reckless to apply the method outside this dataset.

Furthermore, on the basis of the publication of Houston and Galetin (57), it would be inappropriate to conclude that CYP3A4 interactions are fundamentally driven by the total systemic perpetrator concentration, which could lead to an overinterpretation of the mathematical model.

The perpetrator concentration in the intestinal wall during the absorption phase ($[I]_g$) can be described by the following equation [Eq. 25]:

Table 3 Literature analysis of perpetrator concentrations used for predicting DDIs using the MSM or $[I]/K_i$ approach.

| Model | Perpetrators | CYPs involved | Best $[I]$ | References |
|-----------|-------------------------------|--------------------------|---|------------|
| MSM | Competitive MBI Inducer | 3A4 | $[I]_{\text{in,max}}$ (Competitive) $[I]_{\text{u,max}}$ (MBI and inducer) | (27) |
| MSM | Competitive MBI | 3A4, 2D6, 1A2, 2C9, 2C19 | $[I]_{\text{u,max}}$ | (35) |
| MSM | Competitive | 3A4, 2D6, 2C9, 2C19, 1A2 | $[I]_{\text{u,avg}}$ | (55) |
| MSM | MBI | 3A4, 1A2, 2D6, 2C9, 2C19 | $[I]_{\text{u,max}}$ | (34) |
| MSM | Competitive | 2C9, 2D6, 3A4 | $[I]_{\text{avg}}$ | (56) |
| MSM | Competitive | 3A4, 1A2, 2D6, 2C9, 2C19 | $[I]_{\text{u,max}}$ | (15) |
| MSM | Competitive | 3A4 | $[I]_{\text{avg}}$ | (57) |
| $[I]/K_i$ | Competitive | 2C9, 2D6, 3A4 | $[I]_{\text{in,avg}}$ | (8) |
| $[I]/K_i$ | Competitive | 3A4, 1A2, 2D6, 2C9, 2C19 | $[I]_{\text{u,max}}$ | (7) |
| $[I]/K_i$ | Competitive | 3A4, 1A2, 2D6, 2C9, 2C19 | $[I]_{\text{u,max}}$ | (58) |
| MSM | Competitive | 2C9 | $[I]_{\text{u,max}}$ | (59) |
| MSM | Competitive | 3A4 | $[I]_{\text{u,avg}}$ | (60) |
| MSM | Competitive | 2C9, 2C19, 2D6, 3A4 | $[I]_{\text{max}}, [I]_{\text{avg}}$ | (61) |

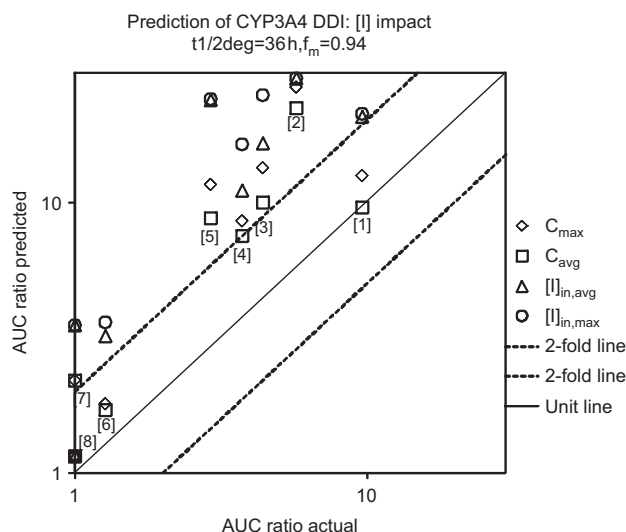


Figure 10 Relationship between the observed AUC ratio *in vivo* and AUC ratio predicted for eight CYP3A4 inactivators (1: clarithromycin, 2: saquinavir, 3: erythromycin, 4: verapamil, 5: diltiazem, 6: fluoxetine, 7: azithromycin, 8: ethinylestradiol).

The plot represents predictions using the average or maximum systemic unbound drug plasma concentration (square or diamond dots, respectively) or the average or maximal inlet hepatic (triangle or circle dots, respectively). The solid line represents line of unity, whereas dashed lines represent the 2-fold limit in prediction accuracy.

$$[I_u]_g = \frac{F_{abs} \times K_{abs} \times D}{Q_g} \quad [25]$$

Non-specific binding

Microsomal binding of drug substrates and/or perpetrators is increasingly recognized as a potential source of artifact arising in the course of *in vitro* studies of drug metabolism. The nonspecific binding of the substrate to a microsomal protein is an important aspect of the extrapolation of *in vivo* drug clearance from data obtained with liver- or recombinantly expressed microsomal systems. These, in turn, may produce inaccurate predictions when *in vitro* data are used to estimate *in vivo* pharmacokinetics (62–67). Inhibitor binding to microsomal systems may likewise influence estimation of potency of metabolic inhibitors (68), resulting in an overestimation of K_i (53, 69, 70). Consequently, *in vivo* hepatic clearance and the extent of inhibitory drug interactions were often underpredicted.

Investigators have tried to use relatively low microsomal protein concentrations to avoid non-specific binding (71). However, relatively high concentrations (1–2 mg/mL) were still needed when studying phase II metabolic reactions (72) and in *in vitro* assessments of the time-dependent inhibition potential (73). As such, it is essential to correct the metabolic kinetic parameters (Cl_{int} , K_m , and K_i) by the unbound fraction to microsomes [$f_{u(mic)}$] to ensure an accurate pharmacokinetic estimation of potential drug candidates.

For drugs, the corresponding $f_{u(mic)}$ values were estimated using the Austin (74) or the Hallifax (75) method. See Eqs. [26] and [27], respectively.

$$f_{u(mic)} = \frac{1}{1 + C \times 10^{0.56 \times \log P/D - 1.41}} \quad [26]$$

$$f_{u(mic)} = \frac{1}{1 + C \times 10^{0.072 \times \log P/D^2 + 0.06 \times \log P/D - 1.126}} \quad [27]$$

where C is the microsomal protein concentration ($g \cdot L^{-1}$), $\log P/D$ is the $\log P$ for basic compounds ($pK_a > 7.4$), and $\log D7.4$ is for neutral or acidic compounds ($pK_a < 7.4$).

Commercial software

Two commercial software packages using the MSM approach have been developed and are currently available in the market. Simcyp population-based Simulator is developed by Simcyp Ltd., Sheffield, UK (<http://www.simcyp.com>), and DDI Predict 2012 Edition is from Aureus Sciences, Paris, France (<http://www.aureus-Sciences.com>).

Even though the mechanistic dynamic model (MDM) approach (see “Mechanistic dynamic model” section) is the cornerstone of the Simcyp population-based Simulator software, it also includes an MSM approach. This MSM approach encompasses all the aspects of metabolism, inhibition, and induction of a drug and also takes advantage of the interindividual variability used extensively in the MDM approach. The features of the compounds of interest (e.g., new compound entities and marketed compounds), considered as inhibitor, inducers, or substrate, are used as input data in the Simcyp software. For marketed compounds, parameters must be obtained from the literature or generated in house. However, some marketed compound parameters are available in the Simcyp library.

DDI Predict 2012 Edition provides a graphical report containing all potential DDIs between a drug candidate and a large panel of marketed or withdrawn drugs. The predictions are supported by calculation of the change in the AUC ratio based on the plasma concentration of drug candidates in the presence or absence of enzyme [CYPs, uridine 5′-diphosphoglucuronosyltransferase (UGTs)] perpetrators. The current version extends the prediction of DDIs to cases where multiple metabolic pathways are inhibited (competitive inhibition and/or MBI) and/or induced. DDI Predict 2012 Edition provides new functionalities, including prediction of fraction metabolized [$f_m(E)$] based on scaling factors (RAF, ISEF, abundance), intestinal metabolism, and others.

To calculate interactions, DDI Predict 2012 Edition uses a large library of drugs (>200 marketed drugs) containing more than 7000 and 8000 inhibition and PK data points, respectively. The use of a large library gains time and provides prediction of DDIs for a large panel of potential comedications.

Mechanistic dynamic model

The MDM refers intrinsically to PBPK models (76, 77). The objective of PBPK is to mathematically describe all physical

and physiological processes that determine a drug's pharmacokinetics. In other words, this type of modeling intends to describe most of the mechanisms involved in the absorption, distribution, metabolism, and elimination of the compound. Conversely, classical PK modeling starts from an *in vivo* concentration time curve. In this case, the experimental data set is used to fit the data into a two- or three-compartment model. Using such a model, a population pharmacokinetic (POPPK) approach provides the identification of covariates (e.g., coadministered drug) explaining part of the variability. For these reasons, covariates are most commonly investigated in parallel to phase III, through a POPPK approach with a large number of patients, with the final dosing schemes and information gathering for drug approval. Before this stage, the observed data are not sufficient to capture all covariates. Nevertheless, the identification and quantification of covariates are not straightforward. Confounding highly correlated covariates can create bias in particular with small or moderate-sized data sets. Low-powered covariates can falsely appear as clinically relevant as they are not mechanistically led but they are selected on a statistical basis (78). This classical approach to modeling has been recently called "top down" (79). In contrast, the bottom-up paradigm (i.e., PBPK models) has also been proposed. PBPK models are derived from the anatomical and physiological structures of the studied organism. They establish a virtual population by building up models integrating physicochemical and metabolic distribution, and *in vitro* parameters of the drug classically generated during the discovery and development processes, using cellular or subcellular models, such as *in vitro* metabolic parameters (K_i , K_m , V_{max} , etc.), mixed with population physiological parameters (tissue structure, tissue composition, tissue volume, and associated blood flow) (Figure 11).

The dynamic model is based on the time course of the concentrations and hence generates a temporal profile of the inhibition process (38, 57). In addition, study design (frequency of administration, dose staggering for DDI, etc.) and clinical conditions (fed or fasted conditions, route of administration, etc.) are taken into account to be mixed with drug and physiologically based pieces of information (Figure 11). The beginning

of this century witnessed a renewed interest in PBPK modeling in the drug development setting, including DDIs (19, 80). The success of this field has been growing in parallel to the availability of the *in vitro* data and the possibility to integrate all these data through a mechanistic model, combined with the power of the computers used to integrate the data (81). PBPK models consider the interplay between physicochemical drug properties, interaction factors between drug and relevant proteins for the administration distribution metabolism and excretion (ADME) fate of the drug, physiological parameters, and clinical trial conditions (e.g., various dosing regimen), in order to simulate individual concentration-time profiles. The use of predictive population modeling allows for a priori assessment of the potential effect of physiological properties and/or the presence of a coadministered drug on the pharmacokinetic parameters of the victim. This effect might be different in a population subgroup (e.g., PM) because of a mixing effect of the perpetrator and the physiological parameters (81). As an example, if a victim is eliminated through the metabolic route through CYP3A4 isoform and renal excretion, the magnitude of the exposure increase in renal impaired subjects coadministered with a CYP3A4 inhibitor can be investigated, allowing the identification of a subgroup of subjects among a given population that are likely to be overexposed.

As a result, patient populations that are likely to be overexposed and thereby considered at risk can be identified even if they are not represented in phase I or II clinical trials, which are conducted with a limited number of healthy subjects or patients.

In early drug development, use of predictive population PBPK models allows for the a priori prediction and interindividual variability without the need for actual *in vivo* data. However, to address DDI using PBPK, it requires two models (with parameters not necessarily available at this stage, see the "MSM vs. MDM" section), one for the victim and one for the perpetrator, which can be time consuming and unreasonable in the discovery stage for a set of development candidates. Once actual human PK data are available from the first-in-man trial, refinement of the model is mandatory and can help in designing clinical DDI in healthy volunteers or specific

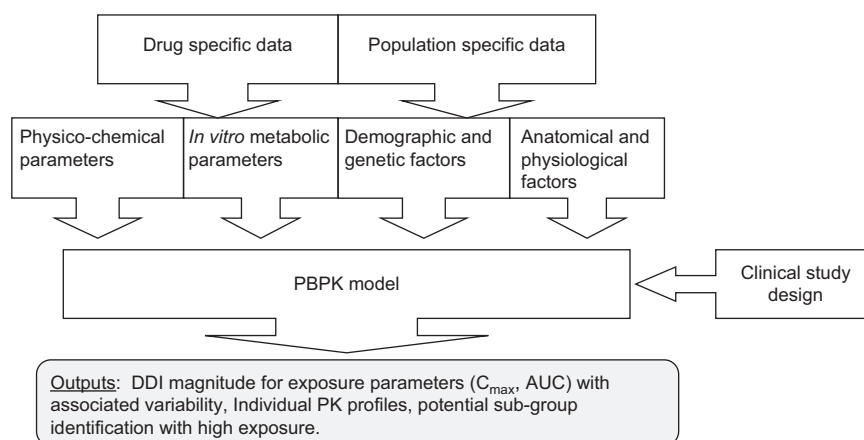


Figure 11 PBPK diagram: drug- and population-specific parameters, used as input data.

populations. PBPK can address several questions during drug development, related to the DDI, through manipulation of the dosages, dose regimen, dose staggering, populations, etc., to predict pharmacokinetic profiles in given clinical conditions.

PBPK modeling offers an improvement on conventional approaches by providing a mechanistic framework for exploring, through computer simulation, the impact of potential sources of variability, including of course DDI, on the likely variation in PK profiles in any part of the body within the target population. This in turn facilitates better design of clinical trials and addresses the likely patient profiles in a whole variety of clinical situations that are unlikely to be evaluated experimentally. Nevertheless, the PBPK approach takes into account a huge number of data pertaining to anatomical and physiological human parameters, molecular properties used for *in silico* predictions, and *in vitro* data used for estimation of parameters characterizing absorption, distribution, and metabolism. Of particular concern is that *in vitro* data, although usually quite reliable from a qualitative point of view, are much less reliable from a quantitative viewpoint. Another limiting factor is the variability in some assay system components. It is essential that accurate estimates of such parameters be made for input into *in silico* models as this information is fundamental for the extrapolation to the *in vivo* situation. All too often, a scientist trawling the literature will encounter a range of values for *in vitro* “constants” such as Cl_{int} , K_m , and K_p , for a given drug, that have been generated under different conditions. Moreover, to capture and quantify the impact of any sources of variability on the exposure of a drug, a complete picture of the ADME features of the drugs (victim and perpetrator) is required. In the case of a perpetrator, the knowledge of circulating metabolites and their inhibitory potency, if any, is crucial as recently shown (61, 82). For a victim, knowledge of elimination pathways (e.g., renal) is crucial for prediction accuracy; the possible saturation of a metabolic pathway, reflected by non-linear pharmacokinetics in the clinic, leads to a level of uncertainty in the predicted magnitude of a DDI (Figure 8). Moreover, all these pieces of information are not known in early development phases and should be used for model refinement along development. Basically, the dynamic model needs to be expanded and refined during drug development and used for accurate prediction once validation has been achieved with actual clinical data. This provides more accurate interaction ratio estimation with linked intersubject variability through assessment of interaction in conjunction with other sources of variability to identify possible outliers. Regarding anatomical and physiological human parameters in particular, there is a need to generate additional and more reliable data, such as those listing changes in blood flow and the composition of individual tissues and organs varying with age, or in interindividual variability in the expression of enzymes and accurate data on genetic and epidemiological factors, in order to generate accurate virtual populations. As an example, virtual population building needs to establish an accurate quantitative relationship between CYP and non-CYP enzyme expression for a better clearance prediction with the best relative involvement prediction of each enzyme,

whereby the individual magnitude in the case of drug interaction should be better assessed, as recently exemplified with correlated expression of CYP3A5 (genetic polymorphic enzyme) and CYP3A4 (83). Another emerging field is the interplay between transporter and enzyme metabolism related to DDIs. For example, this interplay has been shown to influence hepatic clearance and DDI, leading to new challenges in terms of suitable experimental systems and the development of a better understanding of the pharmacokinetic concepts that underpin this interplay (84). In some cases, the required information is currently lacking or poorly assembled, and additional work is needed to accumulate and appropriately assemble the information (85). Hopefully, the volume of these data is increasing everyday in the literature.

Although the PBPK method is not yet officially reported in a final regulatory guidance, it has been extensively described by members of the FDA (86). This recent article reviews examples of the use of PBPK in the decision-making process during regulatory reviews and deals with the use of PBPK to predict the effect of intrinsic (genetics, age, etc.) and extrinsic (DDI) factors or the combination on drug exposures. The authors highlight the usefulness of PBPK along development but also identify several knowledge gaps. Therefore, a validation step is clearly mandatory for regulatory purposes, before claiming, for example, a lack of interaction based on PBPK simulated data.

Several commercial software packages have been developed and are currently available on the market, such as PK-Sim, Gastro-Plus, and Simcyp (non-exhaustive list) (87). All these tools include metabolism- and metabolically based DDI simulations in addition to the other ADME simulated properties, although DDI and metabolism were the initial focus of Simcyp and remain the “core” of this software (81, 88).

Detailed review of the use of PBPK as well as its use during drug development is out of this article’s scope. Readers are invited to refer to good recent reviews on that topic (76, 77, 87, 89, 90).

MSM vs. MDM

Some authors compared MSM and MDM predictive approaches with observed clinical results for a set of interaction ratios, considering only reversible inhibition mechanism (60), reversible and time-based inhibition mechanisms (35), or the two previous mechanisms together with induction (27). MDM was investigated with a PBPK model embedded in the Simcyp software. From a qualitative point of view, out of 100 clinical trials, the two approaches performed well at identifying a potential interaction (AUC ratio ≥ 2 -fold) for a drug vs. a noninteracting drug with around 80% identification rate (35). From a quantitative point of view, 67% and 75% of the studied DDIs were correctly predicted (within 2-fold of the actual value) for MSM and MDM, respectively (35). Among clinical trial interactions with an interaction ≥ 2 -fold ($n=59$), the percentages are 53% and 64% for MSM and MDM, respectively, with a tendency of overprediction for MSM (with

39%) and underprediction for MDM (with 24%). Statistical analysis showed a close value of geometric mean-square error. Notably for MBI, this difference might not be due to the models per se, but more likely linked to the k_{deg} used for modeling, which was different for MSM and MDM, as the magnitude of the prediction is highly dependent on the value of this parameter. Indeed, the authors did not use exactly the same parameter values. In addition to k_{deg} , highly relevant for MBI, some other input data differed between the two models: unbound plasma fraction (f_{up}), intestinal first-pass effect (F_g), and some inhibition constants (K_i) as well as CYP isoform involvement (f_{mCYP}). Therefore, this analysis does not reflect a pure static vs. dynamic comparison per se. Recently, investigations aimed at comparing and evaluating the static and dynamic (PBPK through Simcyp) model approaches for DDI prediction and assessing the impact of including the time course for the inhibition process have been reported (60). A set of 35 DDIs was used where 51% were considered moderate (AUC ratio from 2- to 5-fold), 43% were strong (AUC ratio >5), and the remainder (6%) were weak [from 1.2- to 2-fold with different CYP3A4 inhibitors (ketoconazole, itraconazole, fluconazole) and CYP3A4 victim drugs (alprazolam, triazolam, and midazolam)]. For 40% of the tested DDIs, the difference between the models was minimal: predicted AUC ratios by the static compared with the dynamic method were within 20% of each other. Nearly half of the DDIs showed higher predicted AUC ratios using the static model compared with the dynamic model. In terms of prediction accuracy, 71% and 77% were predicted within 2-fold using the dynamic and static model, respectively. The static model resulted in higher precision and lower bias across the range of DDI potency compared with the dynamic model. A clear underprediction trend (40%) was observed among strong interactions regardless of the model used. The authors identified different accuracies for the models depending on the study design (single vs. repeated dose of the inhibitor) as well as the nature of the inhibitor and/or the substrate themselves. As an example, itraconazole predictions were clearly improved through the dynamic model after inclusion of the time course of the most potent and most abundant metabolite of itraconazole (i.e., hydroxyl-itraconazole), in particular for strong interactions. Surprisingly, the authors did not try to incorporate the metabolite data in the static model, whereas some other authors showed a clear improvement of the prediction accuracy, even using the static model approach, when metabolites were accounted for (61). This conclusion should be put in perspective with another example reflecting the effect of a metabolite that has been described with diltiazem as a perpetrator (82). These authors have also shown the importance of the unchanged compound and the major metabolite of diltiazem at both the liver and gut levels on triazolam (victim drug) exposure after coadministration of these two compounds, through a PBPK model developed by Simcyp. Regarding ketoconazole, for which the inhibitory effect is considered to originate from the unchanged compound only, Guest et al. (60) did not find any benefit from incorporating the time course of the inhibitor with the dynamic model. The authors concluded that no overall significant difference in the prediction accuracy between

the static and dynamic models was found. Generally speaking, the authors highlighted the advantage of the dynamic approach regarding incorporation of intersubject variability and for generating a range of output values whereby the population extremes can be identified. Of note, these investigations were conducted for reversible inhibition of CYP3A4 only. Therefore, the conclusions drawn by the authors cannot be extrapolated to other inhibitory mechanisms (i.e., MBI) and/or other CYP isoforms. MBI with verapamil as the perpetrator and reversible inhibition with ketoconazole as the perpetrator of CYP3A4-mediated substrate metabolism have also been investigated using comparative MDM and MSM approaches (91). The conclusions of these authors are in accordance with others: no major difference in terms of accuracy of the two methods, although PBPK (MDM) enables the simulation of concentration-time profiles and calculation of the related PK parameters, but requires a good understanding of the absorption, distribution, metabolism, and excretion properties of the compounds.

Another comparison was proposed by Fahmi et al. (27) using a mathematical model that simultaneously incorporates reversible inhibition, time-dependent inhibition, and induction of the CYP3A4 isoform (see Eq. [10]). This model, used as mechanistic static model (MSM), was compared with the PBPK of Simcyp (MDM), for 50 *in vivo* clinical trials. In fact, only five drugs exhibited all three interaction mechanisms, among 30 compounds used in the study. For all the others, at least one mechanism pertained to an interaction ratio of unity in the full mathematical model. MSM and MDM correctly predicted DDI (defined as a 2-fold change in exposure) vs. no interaction, in 44 and 45 trials out of the total of 50 trials with a geometric mean square error of 1.74 and 1.47, respectively. Of the trials that had a clinical DDI effect ≥ 2 , the increase in AUC was predicted within 50% of the actual value in 21 and 24 of the trials for MSM and MDM, respectively. Overall, the authors concluded that the static and dynamic models yielded comparable performance in predicting *in vivo* DDIs from *in vitro* data.

However, most MSM models provide point estimates of the average DDI, assuming one precipitant concentration and the same CYP450 enzyme expression levels across the population, whereby the risk to individuals is not evaluated. Nevertheless, an MSM approach incorporating the variability of CYP450 enzyme levels is conceivable, and is addressed with the “steady-state” option in the Simcyp software and is planned to be incorporated in DDI Predict from Aureus Sciences. However, this represents only one source of variability that might be coped with using MSM, whereas MDM is supposed to take into account all the sources (e.g., variability in blood rates) with a time-based approach of predicted concentration allowing the simulation of pharmacokinetic profiles of both perpetrator and victim, with the important interaction C_{max} ratio of the victim. Moreover, as previously mentioned, a computer-simulated program addressing MDM can have the advantage of simulating DDIs in specific populations or patient subgroups (e.g., impaired liver or renal subjects, elderly, or pediatric population) and considering trial design details (e.g., dose staggering, sustained release formulation), whereas

these complex situations are difficult to manage in MSM. This method (MDM) can also cope with the nonlinearity of victim drugs, in particular as concentration of the substrate and K_m values are considered with the full Michaelis-Menten equation, whereas MSM assumes clearance is constant. DDI in subgroups or special populations can be relevant to investigate as some population features can have a dramatic impact, different from “average population,” on the clearance of the victim in presence of the perpetrator. Besides their deterministic features, population-based PBPK models can provide information related to variability of the PK profiles in patient subgroups, as pointed out by authorities (86). The algorithms can take account of the following characteristics of the target population: demographics (gender, age, body size), environmental factors (dietary habits, etc.), genetic differences in enzymes, and potential physiological functions, even if clearly, all the characteristics of these populations that can affect drug interaction are not known. Actually, there is a growing need for information on uncertainty, reflecting, in part the level of confidence in model predictions, and variability, a reflection of the degree to which predictions may differ across a population.

A comparison between MSM and MDM approaches is provided in Table 4. Basically, MSM provides a time-efficient but average estimation of metabolically based DDI magnitude, whereas MDM is intended to provide a subject-based estimation (i.e., intersubject variability, full PK profile). Depending on the question, the development step, and the required accuracy of the answer, the MSM or the MDM approach must be selected appropriately (Table 5). The MDM approach requires detailed pieces of information on metabolism, nonmetabolic elimination pathways, effect of abundant metabolite, overall CYP and other enzymes, and interaction that are available relatively late in drug development. For these reasons, it is sometimes hazardous to use this approach too early in development

(i.e., drug discovery stage) with overabundance of detailed outputs pertaining to variability, population comparison, nonlinearity, relevant sources of variability, and outlier identification, which are totally unbalanced with the input data. These input data are likely not reliable enough at this stage of development and sometimes mixed with the lack of some parameters [e.g., inhibitory effect of an abundant metabolite(s), nonmetabolic elimination pathways, etc.]. Therefore, it is important to consider the overall DDI risk assessment in the context of the quality and availability of the input parameters. In practice, owing to the unavailability of some input data and level of knowledge of the compound, in the first development steps a simple method (MSM) is preferable. Another important consideration is whether it is appropriate and reasonable to dedicate substantial time for setting up PBPK models for each compound among a set of candidates or even leads at the discovery level, at the risk of slowing down the selection process. On the other hand, the MSM approach provides a more “crude” but global and overall risk assessment estimation and is not time consuming. In particular, DDI Predict from Aureus Sciences aims at assessing the DDI risk assessment toward compounds currently in the market (>200) as far as relevant parameters pertaining to the compound as a victim (e.g., f_m) or as a perpetrator (e.g., K_i) are available in the literature. These analyses are conducted very quickly in an automatic manner. Therefore, at the discovery level, a risk assessment can be easily done with several candidates for development, or even earlier. As input data of the evaluated compound, minimal parameters are required (K_i , f_m , etc.) (see related equations provided earlier). DDI risk assessment can be obtained by therapeutic class, with the representative compounds of the class for which enough basic parameters are available in the literature (K_i , f_m , etc.), allowing identification of the highest-risk class in terms of potential DDI, in a semiquantitative

Table 4 MSM and MDM comparison for DDI investigations.

| Type of data | Items | MSM | MDM (PBPK) |
|--------------|---|---------------------|------------------|
| Input | Physicochemical properties of drugs needed | No | Yes |
| | <i>In vitro</i> metabolic data of the drugs needed | Yes | Yes |
| | Distribution data (e.g., f_{up}) needed | Yes | Yes |
| | Time consuming | No | Yes ^a |
| | Metabolite data taken into account | Yes | Yes |
| | Hypothesis for the most relevant [I] needed | Yes | No |
| | | | |
| Output | Magnitude of interaction clearance ratio | Yes | Yes |
| | Investigation of more than one perpetrator | Yes | Yes |
| | Combination of more than one mechanism (e.g., MBI+reversible inhibition) | Yes | Yes |
| | Intersubject variability addressed | Yes/No ^b | Yes |
| | PK profile determination, tissue distribution addressed | No | Yes |
| | Interaction ratios determination for other PK parameters than clearance (e.g., C_{max}) investigated | No | Yes |
| | Covariate impact on interaction (e.g., effect of hepatic impairment on interaction magnitude) addressed | No | Yes |
| | Non-linear PK with time and/or dose of substrate addressed | No | Yes |
| | Complicated study design (e.g., dose staggering) | No | Yes |

^aTwo PBPK models are needed for DDI purpose. ^bNot all variabilities but some of them can be taken into account (e.g., intersubject enzyme abundance variability).

Table 5 Use of MSM and MDM in the drug development setting.

| Development stage | Available parameters used for DDI prediction | Use of MSM | Use of MDM |
|-------------------------|---|--|--|
| • Discovery/preclinical | <ul style="list-style-type: none"> • Inhibitory constant (e.g., K_i) • CYP isoform involvement (e.g., f_m) • Active concentration in relevant pharmacological models | <ul style="list-style-type: none"> • DDI risk assessment toward therapeutic class representatives, to be put in perspective with the intended indication; can be done with several candidates and/or at earlier stages. Therapeutic class ranking according to the risk assessment. | <ul style="list-style-type: none"> • Start building up PBPK for DDI purpose. |
| • Phase I | <ul style="list-style-type: none"> • Collection of pharmacokinetics in healthy volunteers | <ul style="list-style-type: none"> • Use of clinical concentrations for risk assessment refinement, done at different dosages for help of phase II dose selection. | <ul style="list-style-type: none"> • Validation of the PBPK model. • Possible simulation of non-linear PK. • Clinical interaction simulation with probe compounds^a, at different dosages. |
| • Phase II/III | <ul style="list-style-type: none"> • Dose selection and corresponding exposure in patients • PK in special population • Knowledge of elimination pathways of the drug • Outputs of clinical interaction conducted in healthy volunteers, with probe compounds^a | <ul style="list-style-type: none"> • Refinement of the predictions through comparison with clinical data obtained with probe compounds. • DDI risk assessment toward all the compounds likely to be coadministered in phase III trials, in the target patient population. | <ul style="list-style-type: none"> • Refinement of the PBPK model, with observed interaction clinical studies outputs. • Simulations mixing covariates: interaction in special populations (e.g., impaired subjects, poor metabolizers). • Outliers identification. • Predicted PK used for PK/PD simulations. |
| • Submission | <ul style="list-style-type: none"> • Identification of covariates in classical approach (POPPK, “top-down”) | <ul style="list-style-type: none"> • Upon request (from authorities), DDI risk assessment toward additional therapeutic class. | <ul style="list-style-type: none"> • Identification of sources of variability through a “bottom-up” approach, to be put in perspective with the covariates found in POPPK (top-down) modeling. • Use of simulation to avoid conducting interaction studies. • Simulations of unlikely clinical situations to be evaluated experimentally. • Predicted PK used for PK/PD simulations. |

^aProbe compounds refer to drug used as an inhibitor or substrate for a given CYP isoform (e.g., ketoconazole and midazolam as a CYP3A4 inhibitor and substrate, respectively).

approach. At the early stages of development, MSM provides a first insight of the DDI risk toward marketed drugs, as far as relevant parameters can be collected in the literature, which is the case most often, regardless of some compounds developed more than two decades ago. Additionally, for a given therapeutic class, the compounds exhibiting a high risk of DDIs can be identified, which can facilitate the choice of alternative therapeutic compounds to try and mitigate the risk. At this development step, intersubject variability or precise interaction ratios or predictions taking into account other sources of variability are often unnecessary and hazardous, considering the number of unknown parameters for the new compound entity. Additionally, building up PBPK models for such a high number of compounds (candidates, leads, etc.) is not feasible; thus, MDM is not relevant in most cases. A risk assessment from a semiquantitative standpoint (i.e., low, moderate, high) is often enough and more in accordance with the quality and number of parameters, used as input data, known at the early

stages of development. This proposal is also supported by the narrow difference observed between MSM and MDM, in terms of average predicted exposure interaction ratios, by several authors, even from a quantitative point of view (35, 60).

Of course, as previously described, and presented in Table 5, MDM should be used along development in an iterative process with a refinement of the model at each step, for clinical trial simulations, addressing the impact of variability sources and capturing intersubject variability. As the compound progresses to later stages of drug development, PBPK models should be iteratively refined to incorporate additional information on drug disposition from clinical studies in particular (86). This process is also true to a lesser extent for MSM. In addition, simulated pharmacokinetic profiles from MDM can be picked up and in turn integrated in PK/PD modeling to predict any repercussion in pharmacology and/or safety. Late in the development of a drug, such as for submission or even

before, the use of simulation to avoid the requirement to conduct interaction studies with a given victim or perpetrator is helpful, as outliers in a given population are identified, facilitating the documentation of lack of overexposure. Simulations of unlikely clinical situations to be evaluated experimentally can also be simulated at this stage of development.

As illustrated in Table 5, MSM and MDM must be used in a complementary manner depending on the question and the available input data at each discovery/development step.

Conclusions

For the pharmaceutical industry, building a drug interaction plan requires *in vitro* data and mathematical equations to predict the likelihood of significant or high-risk DDI clinical outcomes. However, a complete understanding of the relationship between *in vitro* findings and clinical outcomes of metabolic-based DDIs is still emerging. For inhibition, in particular, representing the most frequent metabolic-based DDI mechanism, the last decade has shown how its mechanism (mechanism-based vs. Michaelis-Menten kinetics) must be accurately addressed to improve the reliability of the prediction model, using the appropriate corresponding equations (15). Increasing understanding of the potential clinical DDI interaction magnitude as soon as possible in discovery stages is imperative for druggability to avoid facing unmanageable clinical DDIs in the late development steps. The Pharmaceutical Research Manufacturers Association has developed and published some years ago a minimal best practices guideline for predicting DDIs for drug development purposes (10). Behind the proposed mathematical equations, two concepts have been recently proposed for DDI prediction (35): MSM and MDM. Basically, the former refers to an “average approach” without taking into account the intersubject variability within a population and cannot consider special populations with modified physiological functions (e.g., impaired hepatic or renal subjects). The time variant change in the concentrations of the perpetrator and the victim are also not considered. This approach essentially lies in the effect toward the clearance of the victim. MDM refers to the PBPK model. The advantages and pitfalls of these two approaches have been detailed in this review. In short, both MSM and MDM must be used through the drug development process in a complementary manner, as they do not require the same level of input data, do not take the same time to perform, do not cope with the same type of simulations, and do not provide the same type of output data. A strategy for the use of both MSM and MDM approaches for a new chemical entity (NCE) is proposed in this review, at each development step, to ensure a reasonable and as reliable as possible DDI risk assessment in conformity with the available parameters, dedicated time, and the requested type of simulated parameters. From a standpoint of average prediction in healthy volunteer populations, large investigations reported in the literature did not show any major difference between the two models in terms of prediction accuracy (35, 60).

Although excellent quantitative concordances of predicted and actual clinical results have been described, in some situations, predictions by both MSM and MDM lead to both over- and underestimations (7, 8, 60). This lack of accuracy is generally attributed to unknown mechanisms (e.g., MBI instead of reversible inhibition, parallel elimination pathways, inhibition due to a metabolite and not the unchanged drug, inhibition or induction of an important cellular transport mechanism, interplay between metabolism and transporters). For example, the unexpected inhibition (based on *in vitro* data to the unchanged compound alone) of cerivastatin CYP2C8-mediated clearance by gemfibrozil has been clearly explained by Shitara et al. (92) who demonstrated that 1-*O*- β -glucuronide of gemfibrozil is a strong CYP2C8 inhibitor through an MBI, but not the aglycone. The example of gemfibrozil is meaningful as the same authors showed as well that the glucuronide inhibits OATP1B-mediated uptake of cerivastatin (90). Gemfibrozil exemplifies the necessity to obtain a complete picture of the *in vitro* results (metabolism and transporter-based in this case) to explain clinical results. Obviously, gemfibrozil clinical outputs have been explained a posteriori, pointing out the lack of knowledge of such mechanisms a priori, in complex situations in most of cases, reflecting that in some cases DDI observed in the clinic is caused by a combination of different DDI mechanisms. Addressing all the possible mechanisms that might be part of the DDI picture for a given compound is certainly the major challenge for the coming years, in order to improve the liability and accuracy of DDI predictions.

Conflict of interest statement

Authors' conflict of interest disclosure: The authors stated that there are no conflicts of interest regarding the publication of this article.

Research funding: None declared.

Employment or leadership: None declared.

Honorarium: None declared.

References

1. Food and Drug Administration. Draft guidance for industry. Drug interaction studies – study design, data analysis, and implications for dosing and labeling. 2006. Available at: <http://www.fda.gov/downloads/Drugs/GuidanceComplianceRegulatoryInformation/Guidances/UCM072101.pdf> (accessed on 23 December 2010).
2. European Medicines Agency. Draft guideline CPMP/EWP/560/95/Rev. 1-Corr. Investigation of drug interactions. 2010. Available at: http://www.ema.europa.eu/ema/pages/includes/document/open_document.jsp?webContentId=WC500090112 (accessed on December 23, 2010).
3. Ito K, Iwatsubo T, Kanamitsu S, Ueda K, Suzuki H, Sugiyama Y. Prediction of pharmacokinetic alterations caused by drug-drug interactions: metabolic interaction in the liver. *Pharmacol Rev* 1998;50:387–412.
4. Bachmann KA. Inhibition constants, inhibitor concentrations, and the predictions of inhibitory drug-drug interaction: pitfalls, progress and promise. *Curr Drug Metab* 2006;7:1–14.

5. Rowland M, Matin SB. Kinetics of drug-drug interactions. *J Pharmacokinet Biopharm* 1973;1:553–67.
6. Beneth LZ, Hoener B. Changes in plasma protein binding have little clinical relevance. *Clin Pharmacol Ther* 2002;71:115–20.
7. Blanchard N, Richert L, Coassolo P, Lave T. Qualitative and quantitative assessment of drug-drug interaction potential in man, based on K_i , IC_{50} and inhibitor concentrations. *Curr Drug Metab* 2004;5:147–56.
8. Ito K, Brown HS, Houston JB. Database analysis for the prediction of in vivo drug-drug interactions from in vitro data. *Br J Clin Pharmacol* 2004;57:473–86.
9. Ito K, Hallifax D, Obach RS, Houston JB. Impact of parallel pathways of drug elimination and multiple CYP involvement on drug-drug interactions: CYP2D6 paradigm. *Drug Metab Dispos* 2005;33:837–44.
10. Bjornsson TD, Callaghan JT, Einolf HJ, Fischer V, Gan L, Grimm S, et al. The conduct of in vitro and in vivo drug-drug interaction studies: a pharmaceutical research and manufacturers of America (PhRMA) perspective. *Drug Metab Dispos* 2003;31:815–32.
11. Venkatakrishnan K, Obach RS. Drug-drug interactions v/a mechanism-based cytochrome P450 inactivation: points to consider for risk assessment from in vitro data and clinical pharmacologic evaluation. *Curr Drug Metab* 2007;8:449–62.
12. Yang J, Liao M, Shou M, Jamei M, Rowland Yeo K, Tucker GT, et al. Cytochrome P450 turnover: regulation of synthesis and degradation, methods for determining rates, and implications for the prediction of drug interactions. *Curr Drug Metab* 2008;9:384–93.
13. Zhang L, Zhang Y, Zhao P, Huang SM. Predicting drug-drug interaction: an FDA perspective. *AAPS J* 2009;11:300–6.
14. Zhang H, Davis CD, Sinz MW, Rodrigues D. Cytochrome P450 reaction-phenotyping: an industrial perspective. *Expert Opin Drug Metab Toxicol* 2007;3:667–87.
15. Obach RS, Walsky RL, Venkatakrishnan K, Gaman EA, Houston JB, Tremaine LM. The utility of in vitro cytochrome P450 inhibition data in the prediction of drug-drug interactions. *J Pharmacol Exp Ther* 2006;316:336–48.
16. Lin JH, Chiba M, Baillie TA. Is the role of the small intestine in first-pass metabolism overemphasized? *Pharmacol Rev* 1999;51:135–58.
17. Paine MF, Hart HL, Ludington SS. The human intestinal cytochrome P450 “pie”. *Drug Metab Dispos* 2006;34:880–6.
18. Paine MF, Khalighi M, Fisher JM. Characterization of interintestinal and intrainestinal variations in human CYP3A-dependent metabolism. *J Pharmacol Exp Ther* 1997;283:1552–6.
19. Rostami-Hodjegan A, Tucker G. ‘In silico’ simulations to assess the ‘in vivo’ consequences of ‘in vitro’ metabolic drug-drug interactions. *Drug Discov Today* 2004;1:441–8.
20. Wang YH, Jones DR, Hall SD. Prediction of cytochrome P450 3A inhibition by verapamil enantiomers and their metabolites. *Drug Metab Dispos* 2004;32:259–66.
21. Galetin A, Hinton LK, Burt H, Obach RS, Houston JB. Maximal inhibition of intestinal first-pass metabolism as a pragmatic indicator of intestinal contribution to the drug-drug interactions for CYP3A4 cleared drugs. *Curr Drug Metab* 2007;8:685–93.
22. Galetin A. Intestinal first-pass metabolism: bridging the gap between in vitro and in vivo. *Curr Drug Metab* 2007;8:643–54.
23. Yang J, Jamei M, Rowland Yeo K, Tucker GT, Rostami-Hodjegan A. Prediction of intestinal first-pass drug metabolism. *Curr Drug Metab* 2007;8:676–84.
24. Yang J, Jamei M, Rowland Yeo K, Tucker GT, Rostami-Hodjegan A. Theoretical assessment of a new experimental protocol for determining kinetic values describing mechanism (time)-based enzyme inhibition. *Eur J Pharm Sci* 2007;26:334–40.
25. Lopez C, Dehance P, Rapine E, Barberan O, Boulenc X. Predictions of metabolic drug-drug interactions after intravenous administration: impact of hepatic extraction ratio. *Drug Metab Rev* 2010;(Suppl 1):151.
26. Fahmi OA, Maurer TS, Kish M, Cardenas E, Boldt S, Nettleton D. A combined model for predicting CYP3A4 clinical net drug-drug interaction based on CYP3A4 inhibition, inactivation, and induction determined in vitro. *Drug Metab Dispos* 2008;36:1698–708.
27. Fahmi OA, Hurst S, Plowchalk D, Cook J, Guo F, Youdim K, et al. Comparison of different algorithms for predicting clinical drug-drug interactions, based on the use of CYP3A4 in vitro data: predictions of compounds as precipitants of interaction. *Drug Metab Dispos* 2009;37:1658–66.
28. Kirby BJ, Unadkat JD. Impact of ignoring extraction ratio when predicting drug-drug interactions, fraction metabolized, and intestinal first-pass contribution. *Drug Metab Dispos* 2010;38:1926–33.
29. Walsky RL, Obach RS. Validated assays for human cytochrome P450 activities. *Drug Metab Dispos* 2004;32:647–60.
30. Walsky RL, Gaman EA, Obach RS. Examination of 209 drugs for inhibition of cytochrome P4502C8. *J Clin Pharmacol* 2005;45:68–78.
31. Walsky RL, Astuccio AV, Obach RS. Evaluation of 227 drugs for in vitro inhibition of cytochrome P450 2B6. *J Clin Pharmacol* 2006;46:1426–38.
32. Fowler S, Zhang H. In vitro evaluation of reversible and irreversible cytochrome P450 inhibition: current status on methodologies and their utility for predicting drug-drug. *AAPS J* 2008;10:410–24.
33. Rodrigues AD. Drug-drug interactions. *Drugs and the pharmaceutical sciences*, 116. New York: Marcel Dekker, 2002.
34. Obach RS, Walsky RL, Venkatakrishnan K. Mechanism-based inactivation of human cytochrome P450 enzymes and the prediction of drug-drug interactions. *Drug Metab Dispos* 2007;35:246–55.
35. Einolf HJ. Comparison of different approaches to predict metabolic drug-drug interactions. *Xenobiotica* 2007;37:1257–94.
36. Grime KH, Bird J, Ferguson D, Riley RJ. Mechanism-based inhibition of cytochrome P450 enzymes: an evaluation of early decision making in vitro approaches and drug-drug interaction prediction methods. *Eur J Pharm Sci* 2009;36:175–91.
37. Galetin A, Burt H, Gibbons L, Houston JB. Prediction of time-dependent CYP3A4 drug-drug interactions: impact of enzyme degradation, parallel elimination pathways, and intestinal inhibition. *Drug Metab Dispos* 2006;34:166–75.
38. Wang YH. Confidence assessment of the Simcyp time-based approach and a static mathematical model in predicting clinical drug-drug interactions for mechanistic-based CYP3A4 inhibitors. *Drug Metab Dispos* 2010;38:1094–104.
39. Silverman RB. Mechanism-based enzyme inactivation, vol. 1. Chemistry and enzymology. Boca Raton, Florida: CRC Press, 1988.
40. Parkinson A, Kazmi F, Buckley DB, Yerino P, Paris BL, Holsapple J, et al. An evaluation of the dilution method for identifying metabolism – dependent inhibitors (MDIs) of cytochrome P450 (CYP) enzymes. *Drug Metab Dispos* 2011;39:1370–87.
41. Kitz R, Wilson IB. Esters of methanesulfonic acid as irreversible inhibitors of acetylcholinesterase. *J Biol Chem* 1962;237:3245–9.

42. Yang J, Jamei M, Rowland Yeo K, Rostami-Hodjegan A, Tucker GT. Kinetic values for mechanism-based inhibition: assessment of bias introduced by the conventional experimental protocol. *Eur J Pharm Sci* 2005;26:334–40.
43. Atkinson A, Kenny JR, Grime K. Automated assessment of the time-dependent inhibition of human cytochrome P450 enzymes using liquid chromatography-tandem mass spectrometry analysis. *Drug Metab Dispos* 2005;33:1637–47.
44. Fahmi OA, Ripp SL. Evaluation of models for predicting drug-drug interactions due to induction. *Expert Opin Drug Metab Toxicol* 2010;6:1399–416.
45. Ohno Y, Hisaka A, Ueno M, Suzuki H. General framework for the prediction of oral drug interactions caused by CYP3A4 induction from in vivo information. *Clin Pharmacokinet* 2008;47:669–80.
46. Crespi CL. Xenobiotic-metabolizing human cells as tools for pharmacological and toxicological research. *Adv Drug Res* 1995;26:179–235.
47. Rodrigues AD. Integrated cytochrome P450 reaction phenotyping: attempting to bridge the gap between cDNA-expressed cytochromes P450 and native human liver microsomes. *Biochem Pharmacol* 1999;57:465–80.
48. Proctor NJ, Tucker GT, Rostami-Hodjegan A. Predicting drug clearance from recombinantly expressed CYPs: intersystem extrapolation factors. *Xenobiotica* 2004;34:151–78.
49. Gibbs JP, Hyland R, Youdim K. Minimizing polymorphic metabolism in drug discovery: evaluation of the utility of in vitro methods for predicting pharmacokinetic consequences associated with CYP2D6 metabolism. *Drug Metab Dispos* 2006;34:1516–22.
50. Venkatakrishnan K, Obach RS. In vitro-in vivo extrapolation of CYP2D6 inactivation by paroxetine: prediction of non stationary pharmacokinetics of drug interaction magnitude. *Drug Metab Dispos* 2005;33:845–52.
51. Ohno Y, Hisaka A, Suzuki H. General framework for the quantitative prediction of CYP3A4-mediated oral drug interactions based on the AUC increase by coadministration of standard drugs. *Clin Pharmacokinet* 2007;46:681–96.
52. Shou M, Hayashi M, Pan Y, Yang Y, Morrissey K, Xu L, et al. Modeling, prediction, and in vitro in vivo correlation of CYP3A4 induction. *Drug Metab Dispos* 2008;36:2355–70.
53. Brown HS, Ito K, Galetin A, Houston JB. Prediction of in vivo drug-drug interactions from in vitro data: impact of incorporating parallel pathways of drug elimination and inhibitor absorption rate constant. *Br J Clin Pharmacol* 2005;60:508–18.
54. Obach RS, Walsky RL, Venkatakrishnan K, Houston JB, Tremaine LM. In vitro cytochrome P450 inhibition data and the prediction of drug-drug interactions: qualitative relationships, quantitative predictions, and the rank-order approach. *Clin Pharmacol Ther* 2005;78:582–92.
55. McGinnity DF, Waters NJ, Tucker J, Riley RJ. Integrated in vitro analysis for the in vivo prediction of cytochrome P450-mediated drug-drug interactions. *Drug Metab Dispos* 2008;36:1126–34.
56. Brown HS, Galetin A, Hallifax D, Houston JB. Prediction of in vivo drug-drug interactions from in vitro data: factors affecting prototypic drug-drug interactions involving CYP2C9, CYP2D6 and CYP3A4. *Clin Pharmacokinet* 2006;45:1035–50.
57. Houston JB, Galetin A. Modelling atypical CYP3A4 kinetics: principles and pragmatism. *Arch Biochem Biophys* 2005;433:351–60.
58. Ito K, Chiba K, Horikawa M, Ishigami M, Mizuno N, Aoki J, et al. Which concentration of the inhibitor should be used to predict in vivo drug interactions from in vitro data? *AAPS Pharm Sci Tech* 2002;4:article 25.
59. Kanamitsu S, Ito K, Sugiyama Y. Quantitative prediction of in vivo drug-drug interactions from in vitro data based on physiological pharmacokinetics: use of maximum unbound concentration of inhibitor at the inlet to the liver. *Pharm Res* 2000;17:336–43.
60. Guest EJ, Rowland Yeo K, Rostami-Hodjegan A, Tucker GT, Houston B, Galetin A. Assessment of algorithms for predicting drug-drug interaction via inhibition mechanisms: comparison of dynamic and static models. *Br J Clin Pharmacol* 2011;71:72–87.
61. Yeung CK, Fujioka Y, Hachad H, Levy RH, Isoherranen N. Are circulating metabolites important in drug-drug interaction? Quantitative analysis of risk prediction and inhibitory potency. *Clin Pharmacol Ther* 2010;89:105–13.
62. Obach RS. The importance of non specific binding in in vitro matrices, its impact on enzyme kinetic studies of drug metabolism reactions and implications for in vitro-in vivo correlations. *Drug Metab Dispos* 1996;24:1047–9.
63. Obach RS, Baxter JG, Liston TE, Silber BM, Jones BC, MacIntyre F, et al. The prediction of human pharmacokinetic parameters from preclinical and in vitro metabolism data. *J Pharmacol Exp Ther* 1997;283:46–58.
64. Obach RS. Non specific binding to microsomes. *Drug Metab Dispos* 1997;25:1359–69.
65. Venkatakrishnan K, von Moltke LL, Obach RS, Greenblatt DJ. Microsomal binding of amitriptyline: effect on estimation of enzyme kinetic parameters in vitro. *J Pharmacol Exp Ther* 2000;293:343–50.
66. Venkatakrishnan K, von Moltke LL, Greenblatt DJ. Application of the relative activity factor approach in scaling from heterologously expressed cytochromes P450 to human liver microsomes: studies on amitriptyline as a model substrate. *J Pharmacol Exp Ther* 2001;297:326–37.
67. Kalvass JC, Tess DA, Giragossian C, Linhares MC, Maurer TS. Influence of microsomal concentration on apparent intrinsic clearance: implications for scaling in vitro data. *Drug Metab Dispos* 2001;29:1332–6.
68. Gibbs MA, Kunze KL, Howald WN, Thummel KE. Effect of inhibitor depletion on inhibitory potency: tight binding inhibition of CYP3A by clotrimazole. *Drug Metab Dispos* 1999;27:596–9.
69. Margolis JM, Obach RS. Impact of nonspecific binding to microsomes and phospholipids on the inhibition of cytochrome P4502D6: implications for relating in vitro inhibition data to in vivo drug interactions. *Drug Metab Dispos* 2003;31:606–11.
70. Tran TH, Von Moltke LL, Venkatakrishnan K, Granda BW, Gibbs MA, Obach RS, et al. Microsomal protein concentration modifies the apparent inhibitory potency of CYP3A inhibitors. *Drug Metab Dispos* 2002;30:1441–5.
71. Jones HM, Houston JB. Substrate depletion approach for determining in vitro metabolic clearance: time dependencies in hepatocyte and microsomal incubations. *Drug Metab Dispos* 2004;32:973–82.
72. Ghanbari F, Rowland-Yeo K, Bloomer JC, Clarke SE, Lennard MS, Tucker GT, et al. A critical evaluation of the experimental design of studies of mechanism based enzyme inhibition, with implications for in vitro-in vivo extrapolation. *Curr Drug Metab* 2006;7:315–34.
73. Soars MG, Burchell B, Riley RJ. In vitro analysis of human drug glucuronidation and prediction of in vivo metabolic clearance. *J Pharmacol Exp Ther* 2002;301:382–90.
74. Austin RD, Barton P, Cockcroft SL, Wenlock MC, Riley RJ. The influence of non-specific microsomal binding on apparent intrinsic clearance, and its prediction from physico-chemical properties. *Drug Metab Dispos* 2002;30:1497–503.
75. Hallifax D, Houston JB. Binding of drugs to hepatic microsomes: comment and assessment of prediction methodology with recommendation for improvement. *Drug Metab Dispos* 2006;34:724–6.

76. Edginton AN, Theil FP, Schmitt W, Wilmann S. Whole body physiologically-based pharmacokinetic models: their use in clinical development. *Expert Opin Drug Metab Toxicol* 2008;4:1143–52.
77. Schmitt W, Wilmann S. Physiology-based pharmacokinetic model: ready to be used. *Drug Discov Today Technol* 2004;1:449–56.
78. Ridding J, Johnsson EN. Power selection bias and predictive performance of the population pharmacokinetic covariate model. *J Pharmacokinet Pharmacodyn* 2004;31:109–31.
79. Jamei M, Dickinson GL, Rostami-Hodjegan A. A framework for assessing inter-individual variability in pharmacokinetics using virtual human population and integrating general knowledge of physical chemistry, biology, anatomy, physiology and genetics: a tale of bottom-up vs top-down recognition of covariates. *Drug Metab Pharmacokinet* 2009;24:53–75.
80. Chien JY, Mohutsky MA, Writon SA. Physiological approaches to the prediction of drug-drug interactions in study populations. *Curr Drug Metab* 2003;4:347–56.
81. Jamei M, Marciniack S, Feng K, Barnett A, Tucker G, Rostami-Hodjegan A. The Simcyp population-based ADME simulator. *Expert Opin Drug Metab Toxicol* 2009;5:211–23.
82. Rowland Yeo K, Jamei M, Yang J, Tucker GT, Rostami-Hodjegan A. Physiologically based mechanistic modelling to predict complex drug-drug interactions involving simultaneous competitive and time-dependent enzyme inhibition by parent compound and its metabolite in both liver and gut. The effect of diltiazem on the time-course of exposure to triazolam. *Eur J Pharm Sci* 2010;39:298–309.
83. Barter ZE, Perrett HF, Yeo KR, Allorge D, Lennard MS, Rostami-Hodjegan A. Determination of a quantitative relationship between hepatic CYP3A5*1/*3 and CYP3A4 expression for use in the prediction of metabolic clearance in virtual populations. *Biopharm Drug Dispos* 2010;31:516–32.
84. Soars MG, Webborn PJ, Riley RJ. Impact of hepatic uptake transporters on pharmacokinetics and drug-drug interactions: use of assays and models for decision making in the pharmaceutical industry. *Mol Pharm* 2009;6:1662–77.
85. Rowland M, Balant L, Peck C. Physiologically based pharmacokinetics in drug development and regulatory science: a workshop report (Georgetown University, Washington, DC, May 29–30, 2002). *AAPS PharmSciTech* 2004;6:article 6.
86. Zhao P, Zhang L, Grillo JA, Liu Q, Bullock JM, Moon YJ, et al. Application of physiologically based pharmacokinetic modelling and simulation during regulatory review. *Clin Pharmacol Ther* 2011;89:259–67.
87. Dong JQ, Gibbs BC, Emery M. Applications of computer-aided pharmacokinetic and pharmacodynamic methods form drug discovery to registration. *Curr Comput Aided Drug Des* 2008;4:54–66.
88. Rostami-Hodjegan A, Tucker G. Simulation and prediction of in vivo drug metabolism in human population from in vitro data. *Nat Rev Drug Discov* 2007;6:140–8.
89. De Buck SS, Mackie CE. Physiologically based approaches towards the prediction of pharmacokinetics: in vitro-in vivo extrapolation. *Expert Opin Drug Metab Toxicol* 2007;3:865–78.
90. Espié P, Tytgat D, Sargentini-Maier ML, Poggessi I, Watelet JB. Physiologically based pharmacokinetics (PBPK). *Drug Metab Rev* 2009;41:391–407.
91. Perdaems N, Blasco H, Vinson C, Chenel M, Whalley S, Cazade F, et al. Prediction of metabolic drug-drug interactions using physiologically based modelling. *Clin Pharmacokinet* 2010;49:239–58.
92. Shitara Y, Hirano M, Sato H. Gemfibrozil and its glucuronide inhibit the organic anion transporting polypeptide 2 (OATP1B1)-mediated hepatic uptake and CYP2C8-mediated metabolism of cerivastatin: analysis of the mechanism of the clinically relevant drug-drug interaction between cerivastatin and gemfibrozil. *J Pharmacol Exp Ther* 2004;311:228–36.